Centro de Alimentación en Investigación y Desarrollo, A.C.

FORMACIÓN DE MATERIALES POROSOS NANOESTRUCTURADOS A PARTIR DE SOLUCIONES DE QUITOSANO EN LÍQUIDOS IÓNICOS BASADOS EN IMIDAZOLIO

_____

Por:

Gonzalo Santos López

TESIS APROBADA POR LA

COORDINACIÓN DE TECNOLOGÍA DE ALIMENTOS DE ORIGEN ANIMAL

Como requisito parcial para obtener el grado de

DOCTORADO EN CIENCIAS

Hermosillo, Sonora   Febrero de 2018

APROBACIÓN

Los miembros del comité designado para la revisión de la tesis de Gonzalo Santos López, la han encontrado satisfactoria y recomiendan que sea aceptada como requisito parcial para obtener el grado de Doctor en Ciencias.
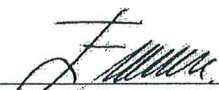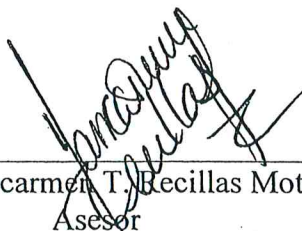
Dr. Jaime Lizardi Mendoza
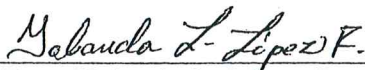Director de Tesis

Dr. Waldo M. Argüelles Monal
Asesor

Dra. Elizabeth Carvajal Millán
Asesor

Dra. Maricarmen T. Recillas Mota
Asesor

Dra. Yolanda L. López Franco
Asesor

DECLARACIÓN INSTITUCIONAL

La información generada en esta tesis es propiedad intelectual del Centro de Investigación en Alimentación y Desarrollo, A. C. (CIAD). Se permiten y agradecen las citas breves del material contenido en esta tesis sin permiso especial del autor, siempre y cuando se dé crédito correspondiente. Para la reproducción parcial o total de la tesis con fines académicos, se deberá contar con la autorización escrita del Director General del CIAD.

La publicación en comunicaciones científicas o de divulgación popular de los datos contenidos en esta tesis requiere la autorización escrita, del manuscrito en cuestión, del director o directora de tesis. En estos casos siempre se deberá dar los créditos al CIAD.

Dr. Pablo Wong González
Director General

AGRADECIMIENTOS

Al personal de la biblioteca del CIAD, Gerardo Reyna Cañez y Luis Conde, por su apoyo en la búsqueda de información.

A cada uno de mis compañeros y amigos del Laboratorio de Biopolímeros y del CIAD: Jorge Marquez, Yaeel Isbeth Cornejo, Damián López Peña, Lilian Mancillas, Daniela González, Ana Luisa Martínez, Daniel Fernández, Daniel Miramón, Rita Paz, Ana Morales, Mayra Méndez Encinas, Alfonso Martínez y José Miguel Fierro.

A mis compañeros y amigos de generación.

Muchas gracias a mi familia.

DEDICATORIA

Dedico esta tesis a mis papás, Virginia López Medina y Gonzalo Santos Soriano. Gracias por apoyarme y brindarme su cariño eterno.

A mis hermanos: Julio, David, Marco, Jonathan y Joshua. Los quiero mucho.

A toda mi familia que me han brindado su confianza y apoyo en cada decisión que he tomado.

A mi fiel compañero, mi canino Aragorn. Solo puedo decirte "wuau".

"Hay hombres que luchan un día y son buenos. Hay otros que luchan un año y son mejores. Hay quienes luchan muchos años, y son muy buenos. Pero los hay que luchan toda la vida: esos son los imprescindibles". Bertolt Brecht

CONTENIDO

CONTENIDO (Continuación)

LISTA DE FIGURAS

LISTA DE TABLAS

RESUMEN

Se estudió el proceso de formación de materiales porosos nanoestructurados de quitosano a partir de soluciones en líquidos iónicos basados en imidazolio. Se realizó la caracterización de las soluciones obtenidas de quitosano en acetato de 1-etil-3-metil-imidazolio y en acetato de 1-butil-3-metil-imidazolio. Se empleó resonancia magnética nuclear de dominio de tiempo para estimar la dinámica de las especies moleculares presentes en las soluciones. Los resultados indican la presencia de, al menos, dos poblaciones de protones en ambientes químicos distintos. Una población de protones de alta movilidad se relaciona con especies de bajo peso molecular, que no son afectadas por la presencia del quitosano. La otra población, en cambio, está conformada tanto por los protones incluidos en el polisacárido como por especies de bajo peso molecular asociados a éste, que presentan menor movilidad y son afectados por la concentración de quitosano. Por otra parte, mediante el análisis reológico se encontró que las soluciones de quitosano en los líquidos iónicos probados tienen un comportamiento de tipo newtoniano cuando su concentración es menor el 1% mientras que a mayores concentraciones se comporta como un fluido pseudoplástico. Las mediciones realizadas permitieron determinar la viscosidad intrínseca del quitosano en ambos líquidos iónicos. Los valores obtenidos son menores a los reportados para quitosano en soluciones ácidas acuosas, lo que indica que la molécula ocupa un menor volumen hidrodinámico al ser disuelta en líquidos iónicos. También se determinó la concentración crítica de solapamiento para ambos tipos de soluciones. La caracterización realizada fue útil para la formación de materiales porosos nanoestructurados, mejor conocidos como aerogeles. Para obtener dichos materiales se formaron geles físicos mediante la difusión de vapor de un agente no solvente, a partir de soluciones de quitosano al 2% (p/p) en cada líquido iónico. Se obtuvieron tres distintos tipos de ionogeles, dos por gelificación empleando etanol y uno más con agua. Los ionogeles producidos con etanol fueron empleados para obtener aerogeles mediante secado con CO_2 en estado supercrítico. Los aerogeles presentaron tamaños de poro entre 31 y 46 nm, y un área superficial específica entre 350 y 480 m^2/g. La estructura interna de los aerogeles se aprecia como una estructura

uniforme formada por cúmulos de masa que forman una red tridimensional compacta con porosidad heterogénea. Este ordenamiento es reflejo de las interacciones que se dan entre el quitosano y el líquido iónico durante el proceso de gelificación.

Palabras clave: quitosano; líquidos iónicos, aerogeles.

ABSTRACT

The formation process of nanostructured porous materials made of chitosan from solutions in imidazolium-based ionic liquids was studied. Solutions of chitosan in 1-ethyl-3-methyl-imidazolium acetate and in 1-butyl-3-methyl-imidazolium acetate were characterized. Time domain nuclear magnetic resonance was used to estimate the dynamics of the molecular species present in the solutions. Results indicate the presence of at least two populations of protons in different chemical environments. In other words, a population of highly mobile protons is related to low weight molecular species, which are not affected by the presence of chitosan. On the other hand, the other population includes the protons of the polysaccharide as well as low molecular weight species associated with it, which have less mobility and are affected by the concentration of chitosan. Additionally, the rheological analysis of the solutions showed that the chitosan solutions in ionic liquids have a Newtonian type behavior when their concentration is less than 1% and, conversely, they behave as a pseudoplastic fluid at higher concentrations. These measurements allowed determining the intrinsic viscosity of the chitosan in both ionic liquids. The estimated values are lower than those reported for chitosan in aqueous acid solutions, which indicates that the molecule occupies a lower hydrodynamic volume when dissolved in ionic liquids. It was also possible to determine the critical concentration of entanglement for both types of solutions. The characterization information was useful for the formation of porous nanostructured materials or aerogels. To obtain such materials, 2% (w/w) chitosan solutions for each ionic liquid were used to produce physical gels by non-solvent agent vapor diffusion. Three different types of ionogels were obtained, two by gelation using ethanol and one more with water. The ionogels produced with ethanol were used to obtain aerogels by drying treatment with CO_2 in the supercritical state. Aerogels have pore sizes in the 31 to 46 nm range and the specific surface area between 350 and 480 m^2/g. The internal structure of aerogels is seen as a uniform structure formed by aggregated clumps forming a compact network with heterogeneous porosity. This structural

13

arrangement result of interactions between the chitosan and ionic liquids during the gelation process.

1. SINÓPSIS

El presente trabajo de tesis está organizado en seis capítulos descritos a continuación. En este primer capítulo se describe la organización del escrito así como el estado del arte que sienta las bases de la investigación. El segundo capítulo se enfoca en la caracterización fisicoquímica mediante resonancia magnética de campo bajo para conocer la dinámica de las soluciones de quitosano en cada uno de los LI seleccionados. En el tercer capítulo se presenta la caracterización reológica del quitosano en los LI para determinar el volumen hidrodinámico que ocupa la molécula. Tanto el segundo como el tercer capítulo corresponden al primer objetivo de la investigación abarcando la caracterización de las soluciones de quitosano en los LI seleccionados. El cuarto capítulo de este trabajo de tesis cubre el segundo y tercer objetivo particular de la investigación, referente a la formación de los geles y aerogeles a partir de las soluciones de quitosano en líquidos iónicos. La obtención de los aerogeles comprendió la formación de geles físicos mediante difusión de vapor de un agente no solvente y su preparación para secarlos con CO_2 en estado supercrítico. La caracterización por medio de espectroscopia de infrarrojo por transformada de Fourier (FT-IR) permitió detectar que los grupos funcionales del quitosano se mantuvieron en los aerogeles. Los materiales tuvieron valores de área superficial específica alrededor de 350 m^2/g y distribución de mesoporos, los cuales son parámetros característicos de los aerogeles. La caracterización por medio del SEM indicó que la estructura interna mostraba una red porosa heterogénea de agregados en ambos tipos de aerogeles. Mediante la realización de experimentos de hinchamiento en el equilibrio se obtuvo que los aerogeles absorben entre 3 y 6 veces su peso en agua, observando una disminución del hinchamiento y de los coeficientes de difusión con la temperatura. En el quinto capítulo se presentan las conclusiones de cada objetivo así como la correlación existente entre cada uno de ellos. Finalmente, el sexto capítulo corresponde a las referencias bibliográficas utilizadas en esta tesis.

Uno de los componentes principales de este tema de investigación es el quitosano, el cual es un polisacárido que ha sido fuente de una gran cantidad de estudios y aplicaciones en áreas como la biotecnología, nanotecnología, ciencias ambientales y biomédicas, entre muchas otras. En la naturaleza es posible encontrarlo formando parte de la estructura de algunos hongos, pero su principal fuente de obtención es mediante el proceso de desacetilación de la quitina. La principal fuente de quitina son los desechos de la industria pesquera, principalmente cáscara de camarón y caparazón de jaiba, a los que se les da un valor agregado. En la naturaleza, la quitina es el segundo polisacárido en mayor abundancia y el primero en tasa de regeneración. A pesar de esto, su aplicación se ve limitada debido a su escasa solubilidad en la mayoría de solventes orgánicos, por lo que su uso principal es como precursor del quitosano. Tanto la quitina como el quitosano pueden ser considerados como variantes de un mismo tipo de moléculas ya que ambos están formados por unidades de N-acetil-glucosamina y D-glucosamina. En el caso del quitosano existen principalmente dos características fisicoquímicas que influyen directamente en su funcionalidad y potencial aplicación: el grado de acetilación (GA) y su peso molecular.

El GA indica la relación entre unidades acetiladas con respecto a las desacetiladas, predominando en el quitosano las unidades desacetiladas (>60%). El quitosano es considerado el único polisacárido natural que presenta un carácter policatiónico. Esto se debe a que en soluciones ácidas acuosas sus grupos funcionales amino son protonados generando un polielectrólito con carga positiva. Esta característica le permite interactuar con distintas moléculas, ya sea por interacciones electrostáticas, puentes de hidrógeno o enlaces covalentes. El GA es de primordial importancia en diferentes funcionalidades del quitosano, como lo es su biodegradabilidad, solubilidad, capacidad de adsorción, bioactividad y biocompatibilidad.

El peso molecular es un parámetro que indica el tamaño de la molécula. Al igual que los polisacáridos conocidos, el quitosano no presenta un peso molecular único, sino que se

refiere a una distribución promedio de pesos moleculares. Es por esto que es considerado un polisacárido polidisperso, ya que presenta distribuciones tanto del peso molecular como del GA, debido principalmente al tipo de fuente del cual se obtiene y las condiciones de su proceso de obtención. Existen propiedades funcionales en las que el peso molecular del quitosano es un factor clave, por ejemplo, en la viscosidad que generan las soluciones, en su bioactividad, en su capacidad para formar materiales, etc. En otros casos, esta influencia es una mezcla tanto del peso molecular y como del GA, siendo estas las dos principales características que influyen en su funcionalidad.

El quitosano es un polisacárido con propiedades funcionales atractivas que van de la mano con sus características fisicoquímicas. Algunas de las principales propiedades funcionales que se le atribuyen son: ser un polisacárido biodegradable, ya que puede ser degradado por diferentes enzimas dando lugar a oligosacáridos no tóxicos; ser un compuesto biodisponible, ya que tiene baja toxicidad y citocompatibilidad en diferentes tipos de células; ser hemostático, mucoadhesivo, fitoestimulante y tener actividad antimicrobiana contra diferentes tipos de levaduras, bacterias y hongos. En el marco de este trabajo de tesis, dos propiedades funcionales del quitosano son consideradas fundamentales: su capacidad estructural y su solubilidad.

La capacidad estructural es una propiedad funcional básica del quitosano. A partir de soluciones de quitosano ha sido posible elaborar distintos tipos de materiales como fibras, materiales tipo esponja, películas, membranas, micro y nanopartículas, hidrogeles y recientemente materiales porosos nanoestructurados, mejor conocidos como aerogeles. Los aerogeles de quitosano son materiales de baja densidad, formados con mesoporos (poros de tamaño entre 2 y 50 nm) y que presentan gran área superficial en un volumen pequeño de material. Las potenciales aplicaciones que se les atribuyen son como materiales para adsorción, soporte, vehículo y transporte de fármacos o diversas moléculas modelo, adsorción y remoción de sustancias contaminantes, como apósitos en el tratamiento de heridas, etc. Al igual que otros polisacáridos el quitosano es no termoplástico, ya que se degrada antes de alcanzar su temperatura de fusión. Debido a esta propiedad es necesario disolver el quitosano en el solvente adecuado, para así poder formar materiales estructurados a partir de sus soluciones.

La solubilidad del quitosano ejerce una importancia clave en sus aplicaciones. El quitosano es insoluble en la mayoría de solventes orgánicos, tradicionalmente se han utilizado solventes ácidos acuosos para disolverlo, como ácidos inorgánicos (ácido clorhídrico, nítrico, bromhídrico, etc.), orgánicos (ácido acético, fórmico, láctico, etc.). La disolución del quitosano en los solventes ácidos acuosos se da por la protonación de los grupos funcionales amino de las unidades desacetiladas, generando repulsiones electrostáticas en sus cadenas poliméricas, favoreciendo el hinchamiento y la separación de las cadenas lo que resulta en una solución verdadera. Además del GA y el peso molecular, hay otros parámetros que se consideran importantes en la formación de las soluciones y son el pH, la fuerza iónica, la adición de un no solvente. Se han reportado solventes alternativos a los solventes ácidos acuosos que pueden disolver al quitosano, como la solución con la sal compleja de formaldehído bisulfito de sodio, el cual genera un quitosano soluble en condiciones neutras. Recientemente se ha reportado que algunos líquidos iónicos (LI) pueden disolver distintos tipos de polisacáridos, entre ellos al quitosano.

Los LI son sales formadas por un catión y un anión que son líquidas a temperatura ambiente. Dos de los LI reportados que logran disolver al quitosano en mayores concentraciones (~ 10% p/p) son el acetato de 1-etil-3-metil-imidazolio (EMIMAc) y el acetato de 1-butil-3metil-imidazolio (BMIMAc). Gran parte de los estudios de estos LI con el quitosano han sido enfocados en la formación de soluciones para la obtención de materiales. Existe un vacío de información con respecto a la caracterización del quitosano disuelto en LI (EMIMAc y BMIMAc). En este trabajo de tesis se pretende aportar al conocimiento parte de la caracterización del quitosano en solución con cada uno de los LI mencionados. Además se busca generar aerogeles a partir de estas soluciones y correlacionar las características estructurales de cada material con las propiedades fisicoquímicas de las soluciones de la cual se forman.

Cs:	Quitosano
Cn:	Quitina
GA:	Grado de acetilación
GD:	Grado de desacetilación
LI:	Líquido iónico
EMIMAc:	Acetato de 1-etil-3-metilimidazolio
BMIMAc:	Acetato de 1-butil-3-metilimidazolio
EMIMCl:	Cloruro de 1-etil-3-metilimidazolio
BMIMCl:	Cloruro de 1-butil-3-metilimidazolio
RMN:	Resonancia magnética nuclear
FT-IR:	Espectrofotómetro de infrarrojo con transformada de Fourier
MBE:	Microscopia de barrido electrónico
M_v:	Peso molecular promedio
M_w:	Peso molecular promedio en peso
Ans:	Agente no solvente
W_{eq}:	Hinchamiento en el equilibrio
W_t:	Cantidad de sustancia difusora que ha entrado o salido en el cilindro al tiempo t
W_{max}:	Cantidad después del tiempo infinito
D:	Coeficiente de difusión aparente
S_{BET}:	Área superficial específica por el método Brunauer-Emmett-Teller
V_p:	Volumen de poro
T_p:	Tamaño de poro

Quitosano

El quitosano (Cs) es un polisacárido que ha servido como molécula modelo debido a sus atractivas características fisicoquímicas y propiedades funcionales. En la naturaleza es posible encontrarlo formando parte del micelio de algunos hongos, como los del género *Mucor rouxxi, Cellototrichum lindemuthianum, Phycomyces blakesleeanus, Absidia coerulea y Rhizopus oryzae,* aunque la principal fuente del quitosano utilizado es a partir del proceso de desacetilación de la quitina (Muzzarelli, 1977; Roberts, 1992). Químicamente el quitosano se constituye por unidades estructurales de 2-acetamida-2-desoxi-D-glucopiranosa (D-glucosamina) y por unidades de 2-amino-2-desoxi-D-glucopiranosa (N-acetilglucosamina) en menor proporción. Cada una de estas unidades se encuentran unidas mediante enlaces covalentes β(1-4) generando un polisacárido con un ordenamiento lineal (Figura 1.) .
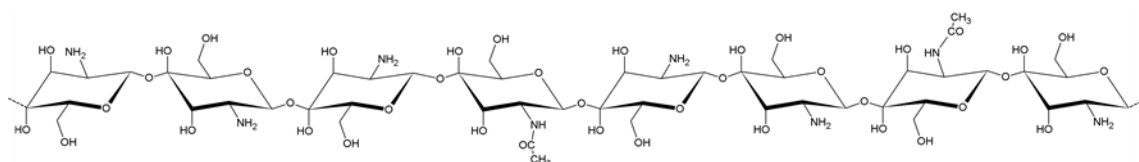
Figura 1. Estructura química del quitosano.

Tanto la quitina (Cn) como el quitosano se pueden considerar como parte de una familia de compuestos con características químicas similares. La principal diferencia radica en la proporción de unidades estructurales, en el caso del Cs predominan las unidades de D glucosamina y en la quitina las unidades de N-acetilglucosamina. Esta diferencia en la proporción de unidades estructurales genera cambios en la funcionalidad de cada uno de estos polisacáridos, como lo es su solubilidad. Son pocos los solventes que disuelven a la quitina, siendo mezclas de compuestos que complican su manejo y aplicación. En cambio, el quitosano tiene un espectro más amplio de solventes en los cuales se puede disolver y llegar a formar soluciones verdaderas, facilitando su remoción y manejo.

Procesos de obtención de quitosano

La quitina, que es la principal fuente de donde se produce el quitosano, es un recurso natural de gran abundancia, estimando una producción anual de 10^{10}-10^{11} toneladas anualmente (Gooday, 1990), solo superadas por la celulosa 10^{11}-10^{12} (Varshney, 2011), aunque la Cn ocupa el primer lugar en la tasa de regeneración. En la naturaleza, la Cn se encuentra formando parte del exoesqueleto de los insectos, del caparazón de crustáceos o formando parte del micelio de hongos. En estas fuentes, la Cn se encuentra en forma de microfibrillas cristalinas ordenadas, siendo parte de matrices complejas que dependiendo de la fuente se pueden encontrar asociadas a componentes como proteínas, sales minerales, pigmentos o lípidos (Muzzarelli, 1977; Roberts, 1992).

Para extraer la quitina de las matrices se siguen una serie de operaciones unitarias que involucran una serie de tratamientos sucesivos, en la mayoría de los casos usando solventes agresivos. Como etapa inicial se separa de la matriz la parte proteica, ya sea por tratamiento enzimático mediante el uso de bacterias proteolíticas o por tratamientos químicos usando medios alcalinos. El siguiente paso es la remoción de minerales mediante el uso de solventes ácidos y, por último, la separación lípidos y/o pigmentos usando solventes con polaridad afín al compuesto a extraer. Como la Cn que se obtiene está formada en su mayoría por unidades acetiladas, es necesario realizar una hidrólisis de estas unidades con el fin de aumentar la proporción de las unidades desacetiladas, típicas del quitosano.

Entre los procesos de desacetilación de la quitina reportados se distinguen principalmente dos tipos de metodologías, las cuales involucran reacciones químicas. Una de ellas es realizando reacciones termoalcalinas en fase heterogénea, en donde la reacción ocurre en las zonas amorfas de las partículas de quitina al interactuar con la solución concentrada de álcali. La otra metodología es la desacetilación homogénea, en la cual a diferencia de la heterogénea, la reacción no es localizada a una zona en específico, si no que se produce de manera uniforme en todos los sitios. En esta técnica se utilizan también soluciones concentradas de álcali a bajas temperaturas pero por

periodos de tiempo prolongados (Goycoolea F., 2004). Existen otros métodos para obtener quitosano a partir de quitina, como utilizar un pre-tratamiento biotecnológico mediante el uso de enzimas del tipo desacetilasas (Beaney, 2005), otro proceso es utilizar irradiación de microondas en condiciones alcalinas para desacetilar la Cn (Sahu, 2009). El tipo de proceso utilizado para obtener el quitosano influye en sus características fisicoquímicas finales, ya que no se generan moléculas con características definidas, si no que se obtienen una distribución de cadenas que varían en el ordenamiento de sus unidades estructurales, composición y tamaño molecular.

Características fisicoquímicas

El quitosano, como la mayoría de los polisacáridos, es polidisperso. Esta variabilidad es atribuida principalmente al tipo de fuente de donde se obtiene y a sus condiciones de procesamiento. Las dos principales características fisicoquímicas del quitosano son el grado de acetilación (GA) y su peso molecular. Los valores indicados de estas características corresponden a una distribución, ya sea de GA o de peso molecular, y no a un valor único como las sustancias de bajo peso molecular.

El GA se refiere a la proporción de unidades acetiladas (N-acetil-D-glucosamina) distribuidas a lo largo de la cadena. Cuando esta es mayor al 40% con respecto a las unidades desacetiladas (D-glucosamina) se le conoce como quitina. De manera inversa se puede expresar esta relación en términos del grado de desacetilación (GD) para clasificar a una muestra como quitina o quitosano. Las principales técnicas que se utilizan para determinar el GA son resonancia magnética nuclear (RMN), el cual es un método absoluto ya que no requiere de alguna calibración con alguna otra técnica (Lavertu, 2003). Una de las técnicas más utilizadas para determinar el GA debido a su sencillez es la espectroscopia de infrarrojo, la cual puede utilizar tanto muestras sólidas como líquidas (Brugnerotto, 2001). Otras técnicas que se utilizan para determinar el GA

son la titulación conductimétrica (Raymond, 1993) y espectroscopia de ultravioleta (Kasaai, 2009).

El peso molecular del quitosano se refiere a una distribución de pesos moleculares. Las técnicas más utilizadas para determinar el peso molecular de una muestra de quitosano en solución son la viscosimetría y dispersión de luz. Mediante viscosimetría se obtiene el peso molecular promedio viscosimétrico (M_v), una de las ventajas es que es una técnica rápida y sencilla de realizar. Otra técnica ampliamente utilizada es la dispersión de luz, la cual es considerada un método absoluto y de donde se obtiene el peso molecular promedio en peso (M_w), en el que la magnitud de la propiedad medida es proporcional a la concentración y tamaño de las partículas presentes (Argüelles-Monal, 2004; Lizardi-Mendoza, 2007).

Propiedades funcionales del quitosano

El GA y el peso molecular son los dos principales parámetros que influyen en la funcionalidad del quitosano. El conocimiento a profundidad de estas características ha permitido controlar y modificar paulatinamente la funcionalidad del quitosano. Las unidades estructurales del quitosano poseen grupos funcionales que le permiten interactuar con diversos tipos de moléculas. En el caso de su disolución en soluciones ácidas acuosas, los grupos amino se protonan con lo que pueden interactuar con otras moléculas ya sea por interacciones electrostáticas, por puentes de hidrogeno, mediante enlaces covalentes. De igual manera las unidades acetiladas pueden generar interacciones con otras moléculas e influir en su funcionalidad.

Algunas de las principales propiedades funcionales de tipo biológicas que se le atribuyen al quitosano son el ser un polisacárido biodegradable ya que puede ser degradado por diferentes enzimas dando lugar a oligosacáridos no tóxicos. También se ha considerado como un compuesto biocompatible y biodisponible dada su baja toxicidad, mostrando además citocompatibilidad en diferentes tipos de células. El quitosano ha probado ser un compuesto hemostático al presentar actividad anticoagulante y mucoadhesivo, ya que

interactúa con la mucosa intestinal. Posee actividad antimicrobiana contra diferentes tipos de levaduras, bacterias y hongos y es fitoestimulante, ayudando al crecimiento de diversas plantas (Aranaz, 2009; Dash, 2011).

Una funcionalidad del quitosano que ha resultado atractiva en diferentes áreas de estudio es su capacidad estructural para poder formar distintos tipos de materiales. Generalmente la quitina y el quitosano se utilizan en forma de hojuelas, las cuales se van moliendo o tamizando para reducir y homogeneizar su tamaño de partícula. Estas hojuelas o polvos en muchas ocasiones tienen la limitante de que las interacciones o reacciones de sus grupos funcionales se dan únicamente en la parte superficial. El quitosano tiene la limitante de que no se puede moldear con temperatura ya que es un polisacárido no termoplástico, por esto la forma de elaborar distintos tipos de materiales es a partir de soluciones de quitosano (Sorlier, 2001). Además del GA y del peso molecular, existen otros parámetros que influyen en las características de los materiales formados, como son la concentración, el tipo de componentes en las soluciones (agentes entrecruzantes, impurezas, solventes, polímeros adicionales en la solución) y las interacciones de estos con el quitosano, además de las condiciones y tipo de procesamiento que se da durante el cambio de fase de las soluciones de quitosano a los nuevos materiales.

Existen distintas metodologías para formar materiales estructurados a partir de soluciones de quitosano, entre ellas destacan la formación de micro y nanopartículas, cápsulas mediante gelificación ya sea de tipo iónica, covalente, mediante interacciones por puentes de hidrogeno, también se han realizado mediante la formación de emulsiones, coacervación-precipitación, etc. (Agnihotri, 2004). En el caso de la formación de fibras se ha utilizado electrospinning (Geng, 2005), también se han podido obtener películas y/o membranas (Argüelles-Monal, 2004). Uno de los materiales ampliamente estudiados son los hidrogeles, los cuales se definen como redes macromoleculares hidratadas caracterizadas por su comportamiento como sólido flexible pese a estar formado en su mayoría por un fluido (Peppas, 1987) y que pueden estar formados mediante interacciones físicas o químicas (Berger, 2004).

Un tipo particular de materiales elaborados a partir de quitosano y que han adquirido gran interés por sus potenciales aplicaciones en distintas áreas son los materiales porosos nanoestructurados, mejor conocidos como aerogeles. Estos materiales se caracterizan por su gran área superficial disponible y tener mesoporos (poros del tamaño entre 2-50 nm). En el caso de aerogeles de quitosano formados a partir de hidrogeles físicos se han reportado materiales con área superficial entre los 120-330 $m^2 \cdot g^{-1}$ y de 66-845 $m^2 \cdot g^{-1}$ para aquellos formados a partir de hidrogeles con entrecruzamientos químicos (Lizardi-Mendoza, 2007; Quignard, 2008). El proceso general utilizado para la elaboración de aerogeles de biopolímeros consiste en remover la fase fluida de geles evitando la deformación de la estructura preformada en medida de lo posible. Esto se logra mediante técnicas de secado que reduzcan al mínimo la tensión superficial de la fase fluida. El proceso más utilizado es el de secado con fluido supercrítico, normalmente CO_2. Inicialmente, a partir de una solución polimérica se forma un gel, al cual se le sustituye su fase fluida por un solvente que sea miscible con el CO_2 (normalmente se usa alcohol o acetona). Este gel se somete a un proceso de secado con CO_2 en condiciones supercríticas (punto crítico: 31.1 °C y 72.8 atm), donde el CO_2 difunde dentro del gel y diluye la fase fluida arrastrándola. Al final del proceso se obtiene un material seco que mantiene en gran parte la estructura original del gel, ya que se evitan los efectos de la tensión superficial en el secado.

Una de las principales propiedades funcionales del quitosano es su solubilidad, ya que a diferencia de la quitina, existen una mayor cantidad de sistemas solventes que pueden solubilizar al quitosano formando soluciones verdaderas. Los solventes con los que se cuenta mayor información del comportamiento del quitosano en solución son aquellos catalogados como solventes ácidos acuosos diluidos, ya sea a partir de ácidos inorgánicos como el ácido clorhídrico, nítrico, perclórico, etc., o también utilizando ácidos orgánicos como el ácido acético, láctico, fórmico, etc. (Roberts, 1992; Argüelles-Monal, 2004). En presencia de estos solventes, los grupos funcionales amino ($-NH_2$) de las unidades desacetiladas del quitosano son protonados, generando repulsiones electrostáticas al interior y exterior de las cadenas poliméricas, provocando la expansión de la molécula lo que provoca a un aumento del volumen hidrodinámico y la solubilidad del quitosano.

En el caso de la disolución del quitosano en ácido acético diluido ocurre el siguiente equilibrio químico (Rinaudo, 1999).

$$CH_3COOH + H_2O \leftrightarrow CH_3COO^- + H_3O^+ \quad (1)$$
$$Cs\text{-}NH_2 + H_3O^+ \leftrightarrow Cs\text{-}NH_3^+ + H_2O \quad (2)$$
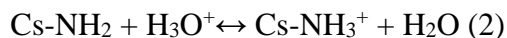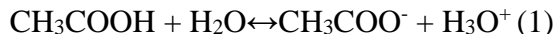
De manera similar, el equilibrio químico que se genera entre el ácido clorhídrico diluido y el quitosano es el siguiente (Rinaudo, 1999):

$$HCl + H_2O \leftrightarrow Cl^- + H_3O^+ \quad (3)$$
$$Cs\text{-}NH_2 + H_3O^+ \leftrightarrow Cs\text{-}NH_3^+ + H_2O \quad (4)$$
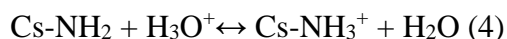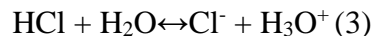
Además de estos solventes ácidos acuosos, también es posible disolver el quitosano con solventes que no involucran interacciones electrostáticas, como por medio de la disolución de la sal compleja de formaldehido bisulfito de sodio (FBS), donde los grupos amino del quitosano interactúan son la sal compleja formando un aducto que resulta en un polielectrólito aniónico capaz de formar soluciones estables en agua a pH neutro (Roberts, 2003; Roberts, 2005). El equilibrio químico de esta reacción es el siguiente:

$$Cs\text{-}NH_2 + HOCH_2SO_3Na \leftrightarrow Cs\text{-}NHCH_2SO_3Na + H_2O \quad (5)$$
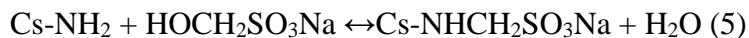
Recientemente ha surgido un conjunto de sistemas solventes que presentan una composición química muy distinta a los sistemas acuosos diluidos que logran disolver al quitosano. Estos solventes carecen de agua en su composición y están formados completamente por iones, conociéndose como líquidos iónicos (LI). Los LI se definen como sales que funden o permanecen líquidas por debajo del punto de ebullición del agua (100 ºC). Su estructura química, generalmente, se compone de un catión orgánico asimétrico de gran tamaño asociado a un anión de tipo mineral u orgánico de menor tamaño (Keskin, 2007). Las principales propiedades fisicoquímicas que presentan la mayoría de los LI son el tener baja presión de vapor, presentar estabilidad química (ya que no generan derivatización por si solos) y tener un amplio rango de estabilidad térmica. Como están formados por iones poseen alta conductividad; además, es posible reutilizarlos una vez recuperados y son compuestos susceptibles de poder modificarlos para alguna aplicación en específico, ya sea modificando el catión y/o el anión (Chen, 2011).

Estas propiedades fisicoquímicas que presentan en su mayoría los LI dependen de su estructura, ya que poseen una región altamente polar debido a su naturaleza iónica, y otro hidrofóbica, que depende del sustituyente alquilo en el anión (El Seoud, 2007). En cambio, las propiedades disolventes de los LI son determinadas principalmente por la capacidad de la sal de actuar como un donador o un aceptor de enlaces de hidrógeno y por el grado de localización de las cargas en los aniones (Keskin, 2007). El estudio de los LI como medios de disolución de polisacáridos es incipiente, siendo gran parte de estos referenciados a materiales celulósicos. Un estudio pionero evidenció la disolución de celulosa en LI basados en el componente 1-butil-3-metilimidazolio (BMIM) como catión y utilizando diferentes tipos de aniones. Se encontró que la combinación del catión BMIM con el ion Cl^- (BMIMCl) fue más efectivo, logrando generar disoluciones hasta en un 25% (p/p) asistido con el uso de microondas como medio de calentamiento. En este mismo estudio se presentó la novedad de poder precipitar la celulosa disuelta en el LI mediante la adición de agua o con otros compuestos como acetona y etanol (Swatloski, 2002). En otro estudio se utilizó este mismo LI para disolver quitina nativa y quitosano, empleando condiciones en las cuales se eliminaba la presencia de agua en el sistema y utilizando temperaturas de 110 ºC controlada mediante un baño de aceite. Bajo estas condiciones se logró alcanzar soluciones con concentración hasta un 10% (p/p) del polímero. La aplicación que se le dio a estas soluciones fue el utilizarlas como agentes de fijación de CO_2 (Xie, 2006).

Otro LI basado en imidazolio que se ha utilizado para formar soluciones de quitina de diversas fuentes (jaiba y pluma de calamar) con patrones cristalinos (β y α) y diferentes pesos moleculares, es el acetato de 1-butil-3-metilimidazolio (BMIMAc). La justificación de parte de los autores de utilizar el ion acetato (Ac^-) en lugar del ion Cl^- se debió a su estabilidad y accesibilidad, ya que tiene mayor capacidad de aceptar enlaces por puentes de hidrógeno. Con el uso de este LI disolvieron quitina de bajo peso molecular hasta en un 6% (p/p) del polímero, pero en el caso de Cn de alto peso molecular obtuvieron soluciones hasta en un 3% (p/p) (Wu, 2008; Qin, 2010). En otro estudio se modificó solamente el catión del LI, utilizando el acetato de 1-etil-3-metilimidazolio (EMIMAc) para extraer quitina directamente del caparazón de camarón, logrando disolver (extraer) a partir de biomasa quitinosa de cáscara de camarón hasta un

46% de masa. Pero no solo eso, sino que al compararlo con los LI de cloruro de 1-etil-3-metilimidazolio (EMIMCl) y BMIMCl, se obtuvieron mayores rendimientos en las soluciones con el LI EMIMAc, tanto de quitina pura (80% de masa) como de quitosano (15.2%) (Qin, 2010). Aunque ya se han logrado formar soluciones de Cn y Cs en los LI a base de metilimidazolio, aún no se ha esclarecido el mecanismo de solubilidad de estos polímeros. La información con la que se cuenta ha permitido generar posibles explicaciones a la influencia que tienen los iones y cationes en la Cn y Cs. Entre lo que se ha explicado es que el componente aniónico de los LI ejerce gran influencia en el proceso de la disolución. Al parecer, aquellos iones que tienen mayor capacidad de disolver a los polisacáridos son los que son buenos aceptores de hidrógeno, tales como los iones de CH_3COO^-, $HCOO^-$, Cl^-, etc.(Wang, 2012). En el caso específico del Cs disuelto en el LI BMIMAc se cuenta con un análisis de la solución al 6% (p/p) mediante RMN de ^{13}C, donde ocurre un desplazamiento químico del carbono del ion acetato, indicando una interacción entre el protón H del grupo amino y/o hidroxilo del quitosano con el oxígeno del grupo carbonilo en el anión CH_3COO^-. Por su parte, en el caso del catión de 1-etil-3-metilimidazol se tiene un mayor desconocimiento de cómo influye en la solubilidad del Cs. Se ha supuesto que existe una fuerte interacción entre el oxígeno del grupo hidroxilo y/o el nitrógeno del grupo amino del quitosano con el carbono del anillo aromático, indicando que tanto el catión como el anión juegan un rol importante en la disolución de quitosano probablemente con el rompimiento de enlaces inter e intra moleculares de hidrogeno (Chen, 2011).

Debido a que los LI EMIMAc y BMIMAc (Figura 2.) se han utilizado para disolver tanto celulosa como Cn y Cs, estos LI se pueden considerar como un medio de miscibilidad para diferentes tipos de polímeros, incrementando sus potencialidades de aplicación (Kuzmina, 2012; Wang, 2013).
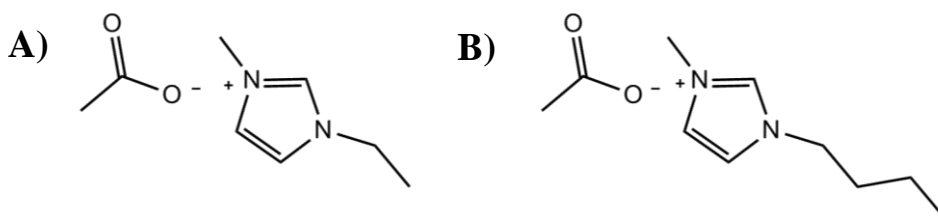
Figura 2. Estructura química del A) EMIMAc y B) BMIMAc.

Referencias bibliográficas

Agnihotri, S. A., Mallikarjuna, N. N. and Aminabhavi, T. M. 2004. Recent advances on chitosan-based micro- and nanoparticles in drug delivery. Journal of Controlled Release 100(1): 5-28.

Aranaz, I., Mengibar, M., Harris, R., Panos, I., Miralles, B., Acosta, N., Galed, G. and Heras, A. 2009. Functional Characterization of Chitin and Chitosan. Current Chemical Biology 3(2): 203-230.

Argüelles-Monal, W., Heras, C. A., Acosta, N., Galed, G., Gallardo, A., Miralles, B., Peniche, C. and San Roman, J. 2004. Caracterización de quitina y quitosano. En: de Abram, A. P. (ed.). Quitina y Quitosano: obtención, caracterización y aplicaciones. Fondo Editorial de la Pontifícia Universidad Católica del Peru Lima, Peru**:** 157-206.

Beaney, P., Lizardi-Mendoza, J. and Healy, M. 2005. Comparison of chitins produced by chemical and bioprocessing methods. Journal of Chemical Technology & Biotechnology 80(2): 145-150.

Berger, J., Reist, M., Mayer, J. M., Felt, O., Peppas, N. A. and Gurny, R. 2004. Structure and interactions in covalently and ionically crosslinked chitosan hydrogels for biomedical applications. Eur J Pharm Biopharm 57(1): 19-34.

Brugnerotto, J., Lizardi, J., Goycoolea, F. M., Argüelles-Monal, W., Desbrières, J. and Rinaudo, M. 2001. An infrared investigation in relation with chitin and chitosan characterization. Polymer 42(8): 3569-3580.

Chen, Q., Xu, A., Li, Z., Wang, J. and Zhang, S. 2011. Influence of anionic structure on the dissolution of chitosan in 1-butyl-3-methylimidazolium-based ionic liquids. Green Chemistry 13: 3446-3452.

Chen, Q., Xu, A., Li, Z., Wang, J. and Zhang, S. 2011. Influence of anionic structure on the dissolution of chitosan in 1-butyl-3-methylimidazolium-based ionic liquids. Green Chemistry 13(12): 3446-3452.

Dash, M., Chiellini, F., Ottenbrite, R. M. and Chiellini, E. 2011. Chitosan--A versatile semi-synthetic polymer in biomedical applications. Progress in Polymer Science 36(8): 981-1014.

El Seoud, O. A., Koschella, A., Fidale, L. C., Dorn, S. and Heinze, T. 2007. Applications of Ionic Liquids in Carbohydrate Chemistry: A Window of Opportunities. Biomacromolecules 8(9): 2629-2647.

Geng, X., Kwon, O.-H. and Jang, J. 2005. Electrospinning of chitosan dissolved in concentrated acetic acid solution. Biomaterials 26(27): 5427-5432.

Gooday, G. W. 1990. The Ecology of Chitin Degradation En: Marshall, K. C. (ed.). Advances in Microbial Ecology. Springer US Boston, MA: 387-430.

Goycoolea F., A. E., Mato R., Ed. (2004). Caracterización de quitina y quitosano. Capítulo 3, *Fuentes y procesos de obtención*. Lima, Peru, Fondo Editorial de la Pontifícia Universidad Católica del Peru.

Kasaai, M. R. 2009. Various Methods for Determination of the Degree of N-Acetylation of Chitin and Chitosan: A Review. Journal of Agricultural and Food Chemistry 57(5): 1667-1676.

Keskin, S., Kayrak-Talay, D., Akman, U. and Hortaçsu, Ö. 2007. A review of ionic liquids towards supercritical fluid applications. The Journal of Supercritical Fluids 43(1): 150-180.

Kuzmina, O., Heinze, T. and Wawro, D. 2012. Blending of Cellulose and Chitosan in Alkyl Imidazolium Ionic Liquids. ISRN Polymer Science 2012: 9.

Lavertu, M., Xia, Z., Serreqi, A. N., Berrada, M., Rodrigues, A., Wang, D., Buschmann, M. D. and Gupta, A. 2003. A validated 1H NMR method for the determination of the degree of deacetylation of chitosan. Journal of Pharmaceutical and Biomedical Analysis 32(6): 1149-1158.

Lizardi-Mendoza, J. 2007. Structured Porous Materials of Chitin and Chitosan. Doctor of Philosophy, Queen's University Belfast.

Muzzarelli, R. A. A. 1977. Chapter 1 - Enzymic synthesis of chitin and chitosan(ed.). Chitin. Pergamon: 5-44.

Peppas, N. A. 1987. Hydrogels in Medicine and Pharmacy: Properties and applications, CRC Press.

Qin, Y., Lu, X., Sun, N. and Rogers, R. D. 2010. Dissolution or extraction of crustacean shells using ionic liquids to obtain high molecular weight purified chitin and direct production of chitin films and fibers. Green Chemistry 12(6): 968-971.

Quignard, F., Valentin, R. and Di Renzo, F. 2008. Aerogel materials from marine polysaccharides. New Journal of Chemistry 32(8): 1300.

Raymond, L., Morin, F. G. and Marchessault, R. H. 1993. Degree of deacetylation of chitosan using conductometric titration and solid-state NMR. Carbohydrate Research 246(1): 331-336.

Rinaudo, M., Pavlov, G. and Desbrières, J. 1999. Influence of acetic acid concentration on the solubilization of chitosan. Polymer 40(25): 7029-7032.

Rinaudo, M., Pavlov, G. and Desbrières, J. 1999. Solubilization of Chitosan in Strong Acid Medium. International Journal of Polymer Analysis and Characterization 5(3): 267-276.

Roberts, G. A. F. 1992. Chitin Chemistry, Macmillan Publishers Limited.

Roberts, G. A. F. (2003). Chitosan condensation products, their preparation and their uses. Nottinghamshire, GB. 20030055211.

Roberts, G. A. F. 2005. A novel solvent system for chitosan, Advances in Chitin Science Vol. VIII. Poznan.

Sahu, A., Goswami, P. and Bora, U. 2009. Microwave mediated rapid synthesis of chitosan. Journal of Materials Science: Materials in Medicine 20(1): 171-175.

Sorlier, P., Denuzière, A., Viton, C. and Domard, A. 2001. Relation between the Degree of Acetylation and the Electrostatic Properties of Chitin and Chitosan. Biomacromolecules 2(3): 765-772.

Swatloski, R. P., Spear, S. K., Holbrey, J. D. and Rogers, R. D. 2002. Dissolution of Cellose with Ionic Liquids. Journal of the American Chemical Society 124(18): 4974-4975.

Varshney, V. K. and Naithani, S. 2011. Chemical Functionalization of Cellulose Derived from Nonconventional SourcesEn: Kalia, S., B. S. Kaith and I. Kaur (ed.). Cellulose Fibers: Bio- and Nano-Polymer Composites: Green Chemistry and Technology. Springer Berlin Heidelberg Berlin, Heidelberg**:** 43-60.

Wang, H., Gurau, G. and Rogers, R. D. 2012. Ionic liquid processing of cellulose. Chemical Society Reviews 41: 1519-1537.

Wang, Z., Zheng, L., Li, C., Zhang, D., Xiao, Y., Guan, G. and Zhu, W. 2013. A novel and simple procedure to synthesize chitosan-graft-polycaprolactone in an ionic liquid. Carbohydrate Polymers 94(1): 505-510.

Wu, Y., Sasaki, T., Irie, S. and Sakurai, K. 2008. A novel biomass-ionic liquid platform for the utilization of native chitin. Polymer 49(9): 2321-2327.

Xie, H., Zhang, S. and Li, S. 2006. Chitin and chitosan dissolved in ionic liquids as reversible sorbents of CO_2. Green Chemistry 8: 630-633.

General

Determinar las propiedades en solución de quitosano en los líquidos iónicos de acetato de 1-etil-3-metilimidazolio y acetato de 1-butil-3-metilimidazolio, así como obtener y caracterizar sus materiales porosos nanoestructurados correspondientes.

Particulares

- Obtener y caracterizar las soluciones de quitosano disuelto en los líquidos iónicos EMIMAc y BMIMAc.
- Obtener y caracterizar los geles formados a partir de quitosano disuelto en los líquidos iónicos EMIMAc y BMIMAc.
- Generar y caracterizar los materiales porosos nanoestructurados de quitosano formados a partir de los líquidos iónicos EMIMAc y BMIMAc.
- Correlacionar las propiedades de quitosano en solución con los líquidos iónicos EMIMAc y BMIMAc con las características morfológicas de sus materiales porosos nanoestructurados correspondientes.

2. ANÁLISIS DE RELAJACIÓN POR RMN-DOMINIO DE TIEMPO DE SOLUCIONES DE QUITOSANO EN EMIMAC Y BMIMAC

Los resultados de este capítulo corresponden al artículo científico titulado:

"TD-NMR relaxation analysis of chitosan dissolution in EMIMAc and BMIMAc"

Se envió a revisión a la revista Soft Matter de la editorial Royal Society of Chemistry.

TD-NMR Relaxation Analysis of Chitosan Dissolution in EMIMAc and BMIMAc

G. Santos-López[a], O. Álvarez-Bajo[b]*, E. Carvajal-Millan[a], Y. L. López-Franco[a], W. M. Argüelles-Monal[a], M. T. Recillas-Mota[a], J. Lizardi-Mendoza[a]*

[a] Grupo de investigación en Biopolímeros. CTAOA. Centro de Investigación en Alimentación y Desarrollo, A.C. Carr. a La Victoria Km 0.6, Hermosillo, Sonora, 83304, México.

[b] CONACYT – CIAD. Carr. a La Victoria Km 0.6, Hermosillo, Sonora, 83304, México.

* Corresponding author. e-mail: jalim@ciad.mx

Abstract

Chitosan, an aminated polysaccharide with distinctive functional properties, can be dissolved in imidazolium based ionic liquids. Even when the dissolution of chitosan in ionic liquids has drove considerable attention and has been used to produce materials intended for application in diverse fields, there still are several aspects of the conformation and molecular dynamics of Cs in such solutions are not comprehensibly described. In order to contribute to the knowledge of this type of solutions the nuclear magnetic resonance proton relaxation parameters of chitosan in 1-butyl-3 methylimidazolium acetate and 1-ethyl-3-methylimidazolium acetate an analysis were analyzed. The obtained data was properly fitted to mono and bi-exponential adjustments. This result could be interpreted as two proton populations, one of them associated to low molecular weight species not substantially affected by the presence of the polymer and other related to molecular species with lower mobility (e.g. polymer molecules). As expected, the temperature modifies the relaxation parameters of both chitosan solutions. At the concentration range tested, the data adjusted properly to the Arrhenius type equation indicating the occurrence of simple thermal process.

Introduction

Chitin is a structural component of the exoskeleton of arthropods (insects, arachnids, myriapods, and crustaceans), a phyla that comprises the most abundant animal biomass. It is a linear polysaccharide, composed of β-(1-4) linked N-acetyl-D-glucosamine (GlcNAc) units, that is chemically similar to cellulose and it is also insoluble in common solvents. The alkaline deacetylation of chitin is a strategy developed to improve its solubility in water [1]. The product of this reaction is chitosan (Cs), where D-glucosamine (GlcN) is the predominant unit forming the polysaccharide (Figure 3). In diluted aqueous acids (pH below 6) the amino moieties in GlcN become protonated, this promote the dissolution of Cs and make it polycationic[2]. Two main characteristic parameters, the molecular weight (Mw) and the degree of acetylation (DA), determine the solubility of chitosan in acid aqueous solvents[1].
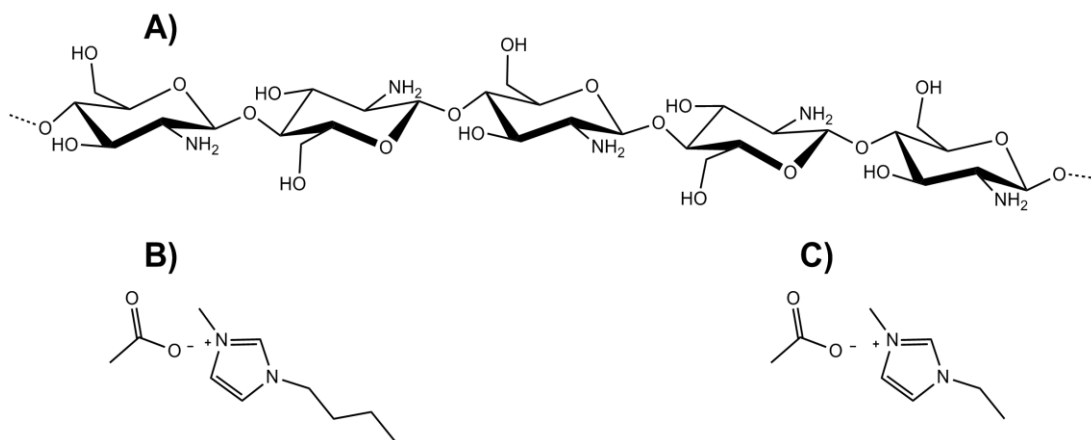
Figure 3. Schematic structure of chitosan (A) BMIMAc (B) and EMIMAc (C).

Chitosan retain most of the structural properties of chitin, but the presence of accessible amino groups along the chain provides it with a unique set of properties among natural polymers. Cs is a biocompatible, biodegradable and abundant renewable resource. It stands out due to remarkable functional properties as: adsorbent (e.g. protein, lipids, pigments and some metals), antimicrobial activity, phytostimulant and diverse effects of biomedical interest (e.g. hemostatic, wound healing promoter, hypocholesterolemic, transfection vector, etc.)[1,3,4]. However, since chitosan is not thermoplastic, it is necessary

36

to obtain Cs solutions or stable colloidal dispersions to produce materials. Despite many Cs applications have been developed from acid solutions there are opportunity areas for alternative solvents that allow the dissolution of Cs in neutral, alkaline or organic media. This could derive to innovative chitosan structures, composites and applications. The ionic liquids (IL) belong to a novel class of solvents that have generated interest as greener substitutes for traditional volatile organic solvents, due to their unique physicochemical properties like low vapor pressure, low melting point and stability in a wide range of temperature5. The dissolution of polysaccharides in IL has been reported mainly focused on the dissolution of cellulose[6–8]. The effective dissolution of chitosan in 1-butyl-3-methylimidazolium chloride (BMIMCl), was first reported by Xie and collaborators [9]; subsequently there are several mentions in literature using IL as solvents for chitosan[10–12]. Additionally, the influence of the structure of ILs on the chitosan dissolution performance and possible dissolution mechanism has been explored[10,11,13]. In contrast, the dissolution of Cs in aqueous acids has been widely studied [2,14–16]. In this type of solutions Cs adopts a conformation usually described as semi-rigid polymer that highly dependent on the balance between two possible contrasting effects: the electrostatic repulsion between adjacent protonated amino groups and the steric hindrance associated to the bulkier acetamido groups [2,15]. It is assumed that these effects do not prevail for Cs solutions in IL; however, several aspects of the conformation and molecular dynamics of Cs in such solutions are not comprehensibly described yet.

The time domain nuclear magnetic resonance (TD-NMR) is a powerful tool for the study of the dynamic and flexibility of macromolecules. This is one of the well-known techniques for studying the rotational reorientation of ions and molecules in various liquid system[17]. The main measurable parameters, longitudinal (T_1) and transverse (T_2) relaxation times, provide valuable information about the molecular motion [14,17]. Therefore, TD-NMR experiments were used to study Cs solutions in 1-ethyl-3-methylimidazolium acetate (EMIMAc) and 1-butyl-3 methylimidazolium acetate (BMIMAc) at several concentrations and temperatures in order to contribute to the knowledge on the molecular conformation and dynamics of chitosan in IL solutions.

Methods

Materials. Reagent grade ionic liquids, EMIMAc (90%) and BMIMAc (95%), were acquired from Sigma Aldrich. The IL were stored in desiccator at room temperature until use. Pandalus borealis shrimp shell chitosan (batch No. TM 1961) was provided by Primex EHF (Iceland). The main chitosan parameters were DA = 16.3%, determined by ^{13}C NMR and Mw = 201.3×10^3 g/mol, measured by dynamic light scattering. Prior its use, Cs was purified as follows. A diluted solution of Cs (0.5 % wt in 0.3 M acetic acid) was filtered stepwise through 8, 3, 1.2, 0.8 µm cellulose membranes, then neutralized with 10% NaOH up to pH 8. The precipitated Cs was recovered, washed thoroughly with ethanol/water mixtures and freeze-dried.

Dissolution of chitosan in IL. Each IL was kept 24 h in a vacuum oven at 110 °C before use it. Batch solutions at the highest concentration were prepared as follows. The IL was transferred to a round bottomed flask that was filled with nitrogen gas and heated to 110 °C in an oil bath. Then, Cs was added in portions of 0.2% wt, waiting for complete dissolution before adding the next portion, until the final concentration (3.0% wt) was reached. Solutions of different concentrations were prepared by dilution from their respective stock solutions.

TD-NMR experiments. A Bruker Minispec MQ20 NMR spectrometer was used to measure the proton relaxation times, T_1 and T_2, of the Cs solutions in IL. A standard inversion-recovery pulse sequence was used for the T_1 detection. The control parameters for these experiments were recycle delay (RD) of 1.5 s with initial inversion recovery delay (IR Delay) of 5 ms; each experimental run consisted in four scans collecting 32 points each. On the other hand, T_2 measurements were done using a Carr-Purcell pulse sequence with pulse separation of 1 ms with eight scans. A recovery delay between scans of 15 minutes was set for all TD-NMR experiments. The reported values of T_1 and T_2 are average values of five measurements with estimated uncertainties smaller than 5% in all cases.

Results and Discussion

The T_1 relaxation time represents the energetic exchange between excited nuclear spins and the lattice. The spin-lattice relaxation can occur by several mechanisms including chemical shielding anisotropy, spin rotation, quadrupole interactions and others. However, the proton dipolar interaction between neighboring protons is the main relaxation pathway. This is particularly relevant in polymeric systems, therefore, spin-lattice relaxation time is commonly used as a quasi-quantitative indicator of the relative motion of the chain[18]. Such motion accounts from molecular tumbling (related to the system viscosity) and segmental movement up to functional groups and atoms rotations or vibrations. For its part, the T_2 (transverse) relaxation time represent the direct interaction between spins influenced by effects of fluctuating magnetic fields [19,20]. Normally, the spin-spin interactions determine the T_2 without affecting the net magnetization in the z directions (T_1) because the spin exchange occurs adiabatically (i.e. without energy transfer to the lattice). For water and other solvents T_1 is normally larger than T_2. Similarly, the measured T_1 of BMIMAc and EMIMAc were higher than T_2 in all the experimental conditions.

Relaxation Data Analysis: CsBMIMAc. The behavior of spin lattice relaxation (T_1) of the CsBMIMAc solution at different concentrations and temperatures is included in Figure 2a. At the lower tested temperatures T_1 is independent of the Cs concentration. Over 40 °C a slight decrease of T_1 could be observed when Cs go over 1% concentration. This has been related to increasing steric hindrance to the sectional motions that comes from the interaction between polymer molecules (intermolecular interactions) [21].
For polymer solution T_1 is usually larger than T_2 [14,18]. The same has been observed in CsBMIMAc (Figure 4.). However, the difference between them is reduced noticeably at higher temperatures. Conversely, there is some decrease of T_2 as result of the rise of Cs concentration. It is noticeable that T_2 is more sensible to temperature and Cs concentration change than T_1. This could be related to the significant contribution to T_2
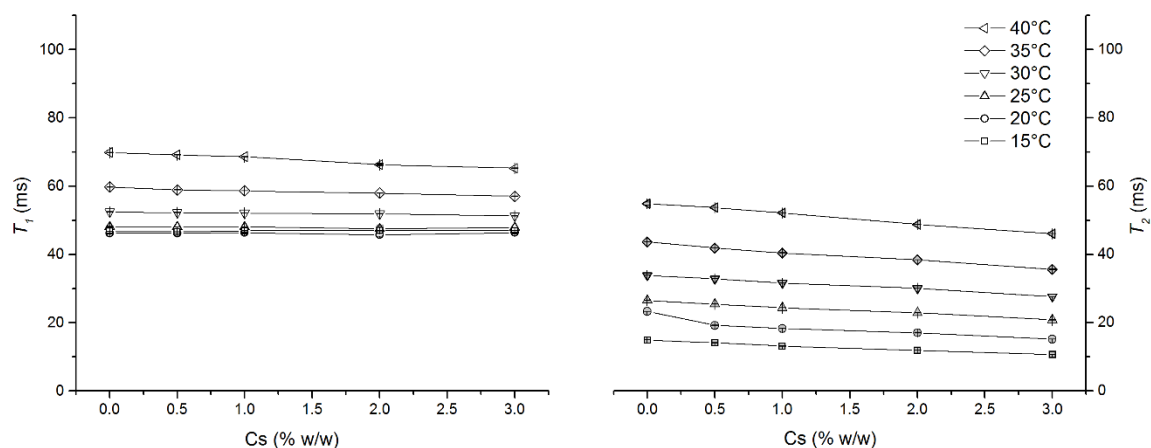
Figure 4. Cs BMIMAc T1 and T2 vs Concentration.

of slower long-range motions that are hindered by an increase in viscosity and chain entanglement to greater extent than the segmental motions[18].

The experimental data were also fitted to a bi-exponential adjustment obtaining two component relaxation times (Figure 5.). The components of T_1 display dissimilar behavior. While T_{1a} (Figure 5a) increase with the temperature and decrease with concentration, which is more evident at Cs concentrations higher than 1%; T_{1b} (Figure 5b) is independent of the concentration and the effect of the temperature is lower. Conversely, both components of T_2 (T_{2a} and T_{2b}; Figure 5c and 5d, respectively) behave similarly, decreasing with the concentration and increasing with the temperature. These observations could be related to two proton populations in distinct chemical environment. One proton population is associated to low molecular weight species with short relaxation times that are not substantially affected by the presence of the polymer. The other proton population is related to molecular species with lower mobility, either polymer molecules or solvent moieties in close interaction with them.
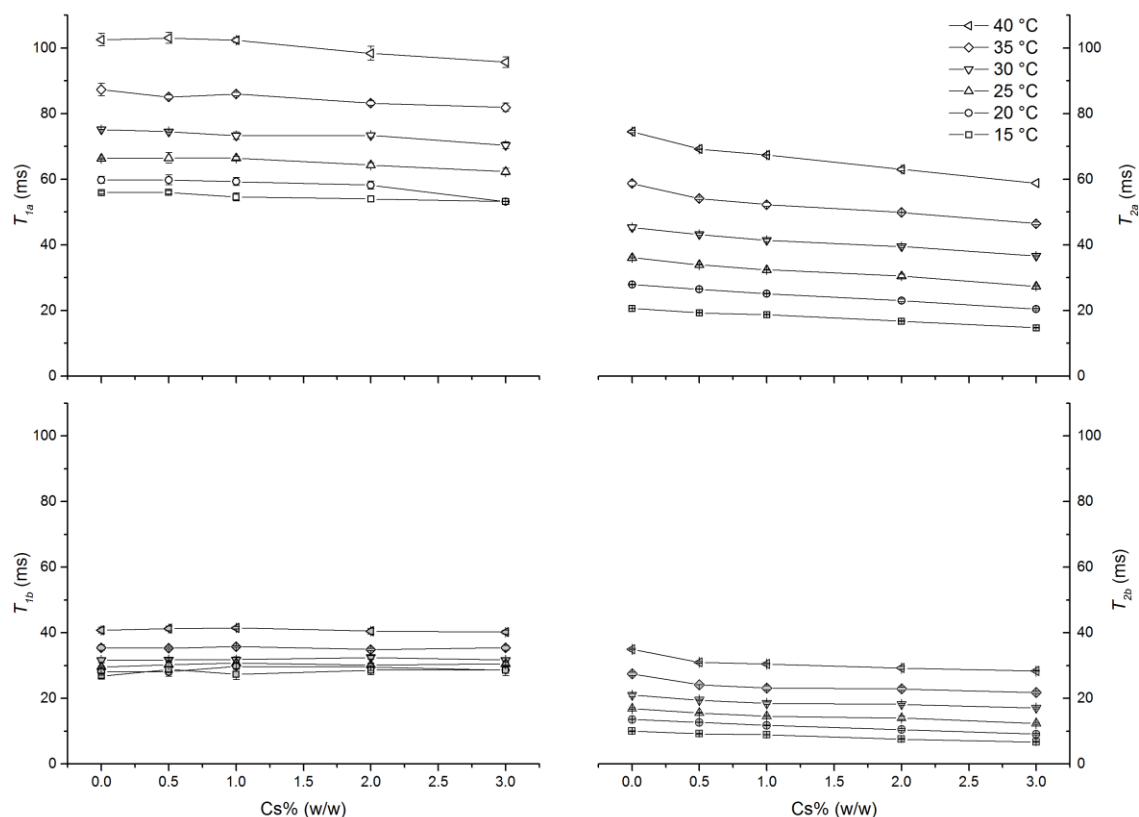
Figure 5. Cs BMIMAc relaxation times from bimodal adjust on dependence of concentration and temperature.

CsEMIMAc. The relaxation times for Cs solutions in EMIMAc are included in Figure 6. both T1 and T2 rise with the temperature. In contrast, T1 decrease with Cs concentration, but T2 remains constant up to 1% Cs then decrease with further increments in concentration. This behavior is more evident at higher temperatures. In general, the relaxation parameters of CsEMIMAc are larger compared to those of CsBMIMAc. Shorter relaxation times are related to higher number and type of molecular interactions. Thus, the observed results are consistent with studies that point out BMIMAc as the best imidazolium-based solvent for chitosan[10,11,21].
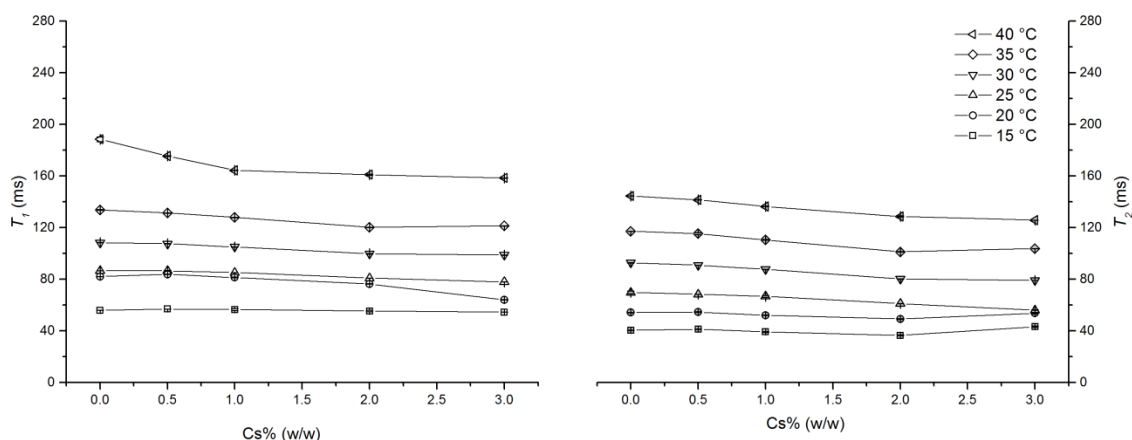
Figure 6. Cs EMIMAc relaxation times in function of concentration and temperature.

The results of bi-exponential adjustment for Cs EMIMAc data are included in Figure 7. The general behavior was similar to the observed for CsBMIMAc with one of the components of both relaxation time parameters less affected by the presence of the polymer in the solution. The components with longer relaxation times (T_{1a} and T_{2a}) are reduced as the Cs concentration rise, being this more notorious at higher temperatures. For this solution, irregular data behavior was observed at the highest temperature and Cs concentration tested. It has been noted that NMR relaxometry is sensitive to self-association (i.e aggregation) processes occurring in solution [22]. Taking this in account and considering that EMIMAc is a relatively poorer solvent of chitosan, the measurements could be affected by incipient chitosan aggregation. Unusual self-association of this polysaccharide (not based on hydrogen bonding nor polar interactions) has been observed previously [23].
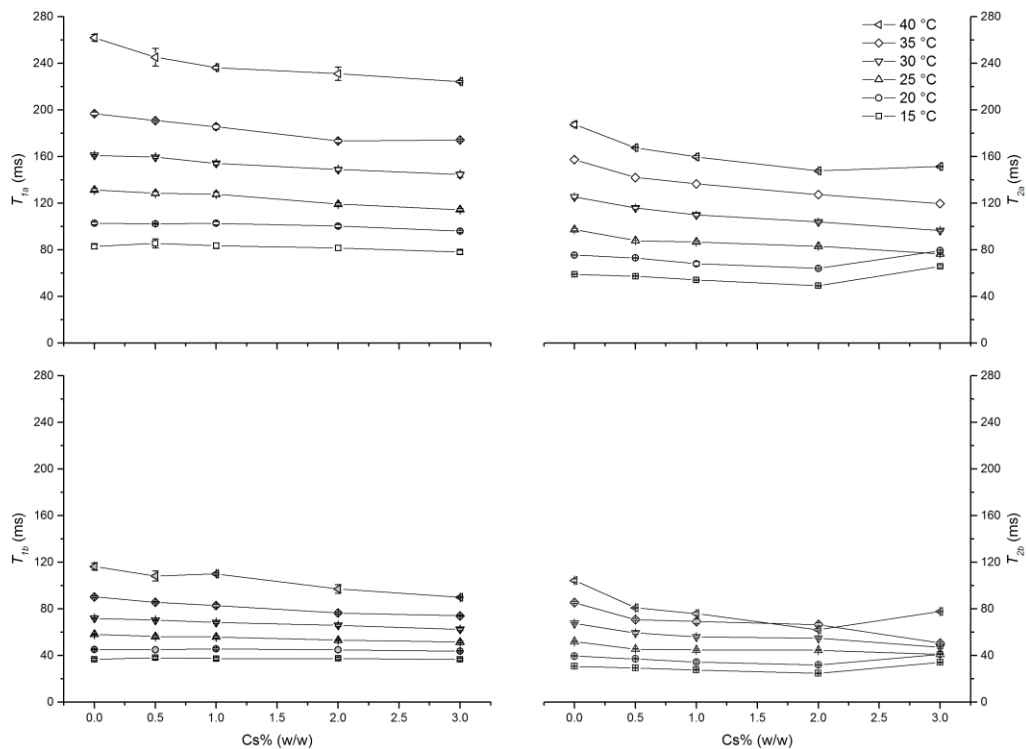
Figure 7. Cs EMIMAc relaxation times from bimodal adjust on dependence of concentration and temperature.

Usually, T_1 is considerably larger than T_2 in polymeric solutions [18]. However, for Cs solutions in imidazolium based IL is noticeable that the observed relaxation times are similar, even when T_1 is higher than T_2 in all the cases. The ionic interactions in the solvents and the viscosity of the solution may contribute to reduce the difference among T_1 and T_2. The relevance of such interactions is also observed in the contrast with the relaxation parameters of Cs solutions in diluted acid, where T_1 is independent of the Cs concentration [14].

Effect of temperature on relaxation parameters. To further investigate on the role of the temperature over the proton relaxation parameters of the Cs solutions in IL an Arrhenius type analysis was performed. The motional process response to increasing temperature was adjusted to following equation:

$$T_n = A \exp\left(\frac{-E_a}{R\mathrm{T}}\right) (6)$$

43

Where 'T_n' can be T_1 or T_2, 'A' is a fitting factor, 'E_a' is the activation energy of the narrowing process, 'R' is the gas constant and 'T' is the temperature.

NMR motional narrowing take place when the fluctuation of the local magnetic fields are comparable with rigid-lattice line widths[24]. This may be due to either exchange interactions resulting from intermolecular collisions or dipole-dipole interactions. From this, the T_1 is mainly related to molecular reorientation motions increasing with the temperature due to thermal disorder. Therefore, T_1 is sensitive to the faster moving molecules (short range order) resulting in good Arrhenius type fitting over the investigated temperature range, indicating a single motional mode. Conversely, T_2 is dominated by long range order changes affected by the temperature. These changes could result of the altered motion of the molecular species in the solution and aggregation processes, rendering long-range ordering less probable in comparison to short range ordering once thermal motion began to dominate.

The data of both chitosan solutions adjusted properly to the Arrhenius type equation, indicating that simple thermal process occurs in the tested concentration range. In general, T_1 and T_2 increase with the temperature (Figure 8. and 9.); however, the effect on T_1 is greater for CsEMIMAc, conversely the effect on T_2 is slightly higher for CsBMIMAc. The Ea of the relaxation parameters of the solvents were affected by the presence of chitosan in the solutions (Table 1.). For the CsBMIMAc the reduction of Ea of both relaxation times is apparently linear with the increase of chitosan concentration. On the other hand, for CsEMIMAc no clear tendency was observed, even when there is a reduction of Ea with the presence of chitosan. The activation energy has been related with a chemical exchange between solvent protons and labile polymer protons[25,26].

44
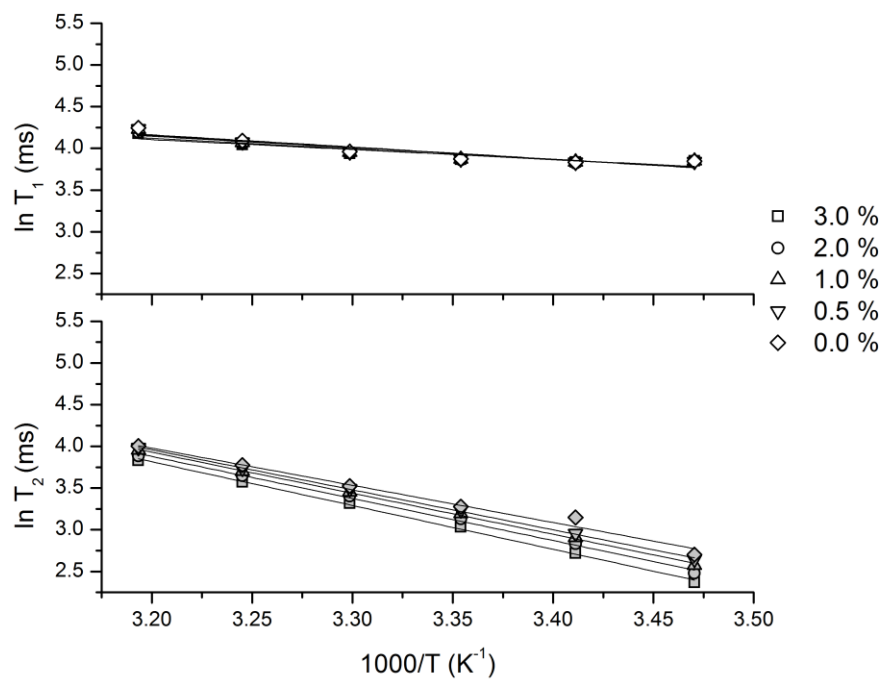
Figure 8. Arrhenius type plot of time decays as a function of inverse temperature of CsBMIMAc. Continuous lines arise from Arrhenius fitting.
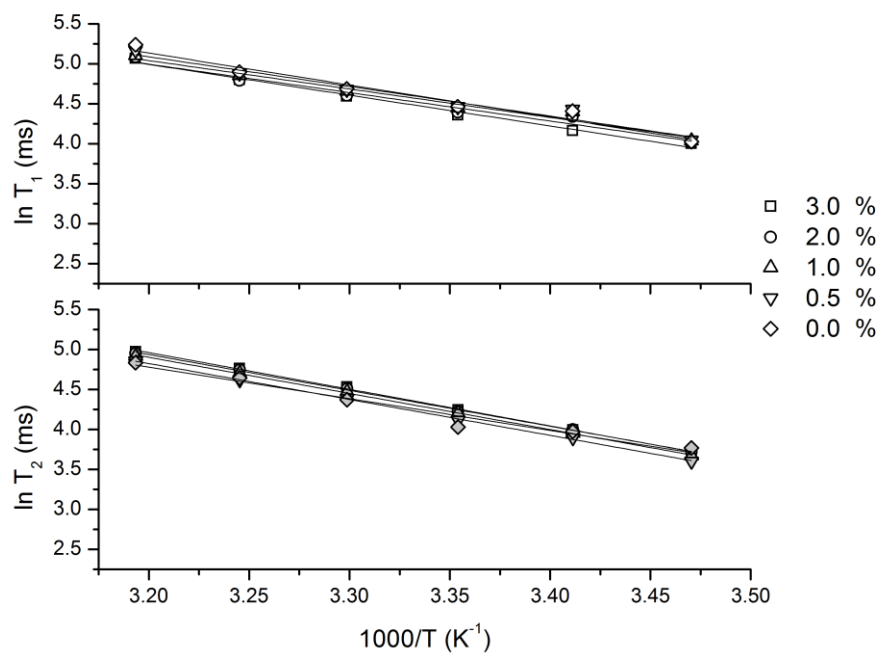
Figure 9. Arrhenius type plot of time decays as a function of inverse temperature of CsEMIMAc. Continuous lines arise from Arrhenius fitting.

Table 1. Activation energies for chitosan dissolved in BMIMAc or EMIMAc at different concentrations.

[Cs] % (w/w)	Ea (kJ·mol⁻¹)	
	T_1	T_2
BMIMAc		
0	12.15 ± 2.51	43.65 ± 0.92
CsBMIMAc		
0.5	11.84 ± 2.44	41.92 ± 1.11
1.0	11.39 ± 2.45	40.94 ± 0.70
2.0	10.68 ± 2.33	39.85 ± 0.48
3.0	9.90 ± 2.15	37.09 ± 2.39
EMIMAc		
0	33.23 ± 3.12	38.12 ± 0.56
CsEMIMAc		
0.5	30.82 ± 2.95	37.27 ± 0.62
1.0	29.56 ± 2.52	37.56 ± 0.50
2.0	29.55 ± 2.50	37.38 ± 0.54
3.0	31.99 ± 1.56	32.81 ± 2.97

Conclusions

The analysis of the proton relaxation parameters allow further insight on the molecular behavior of Cs in imidazolium based IL (BMIMAc and EMIMAc). The T1 was higher than T2 in both solutions; however, the difference between them is minor compared with the difference observed for Cs solutions in aqueous acids. In general, the relaxation times of the CsBMIMAc were reduced proportionally with Cs concentration increase. For CsEMIMAc, such reduction becomes evident at Cs concentrations over 1%. In both cases, the data were also properly fitted to a bi-exponential adjustment, the higher component was more influenced by Cs concentration. This result could be interpreted as two proton populations, one of them associated to low molecular weight species not substantially affected by the presence of the polymer and other related to molecular species with lower mobility (e.g. polymer molecules). As expected, the temperature modify the relaxation.

References

1   J. Lizardi-Mendoza, W. M. Argüelles Monal and F. M. Goycoolea Valencia, in *Chitosan in the Preservation of Agricultural Commodities*, eds. Silvia Bautista-Baños, G. Romanazzi and A. Jiménez-Aparicio, Academic Press, San Diego, 2016, pp. 3–31.

2   M. Rinaudo, G. Pavlov and J. Desbrières, *Polymer*, 1999, **40**, 7029–7032.

3   M. Dash, F. Chiellini, R. M. Ottenbrite and E. Chiellini, *Prog. Polym. Sci.*, 2011, **36**, 981–1014.

4   M. Rinaudo, *Prog. Polym. Sci.*, 2006, **31**, 603–632.

5   K. R. Seddon, *J. Chem. Technol. Biotechnol.*, 1997, **68**, 351–356.

6   A. Benedetto and P. Ballone, *ACS Sustain. Chem. Eng.*, 2016, **4**, 392–412.

7   H. Liu, K. L. Sale, B. M. Holmes, B. A. Simmons and S. Singh, *J. Phys. Chem. B*, 2010, **114**, 4293–4301.

8   R. C. Remsing, G. Hernandez, R. P. Swatloski, W. W. Massefski, R. D. Rogers and G. Moyna, *J. Phys. Chem. B*, 2008, **112**, 11071–11078.

9   H. Xie, S. Zhang and S. Li, *Green Chem.*, 2006, **8**, 630–633.

10   X. Sun, Q. Tian, Z. Xue, Y. Zhang and T. Mu, *RSC Adv.*, 2014, **4**, 30282–30291.

11   Q. Chen, A. Xu, Z. Li, J. Wang and S. Zhang, *Green Chem.*, 2011, **13**, 3446-3452.

12   Y. Chen, X. Sun, C. Yan, Y. Cao and T. Mu, *J. Phys. Chem. B*, 2014, **118**, 11523–11536.

13   B. Xu, Q. Li, L. Zhuang, Q. Wang, C. Li, G. Wang, F. Xie and P. J. Halley, *Fibers Polym.*, 2016, **17**, 1741–1748.

14   R. Novoa-Carballal, E. Fernandez-Megia and R. Riguera, *Biomacromolecules*, 2010, **11**, 2079–2086.

15   M. Rinaudo, M. Milas and P. L. Dung, *Int. J. Biol. Macromol.*, 1993, **15**, 281–285.

16   W. Wang, S. Bo, S. Li and W. Qin, *Int. J. Biol. Macromol.*, 1991, **13**, 281–285.

17   V. V. Matveev, D. A. Markelov, E. A. Brui, V. I. Chizhik, P. Ingman and E. Lähderanta, *Phys. Chem. Chem. Phys.*, 2014, **16**, 10480–10484.

18   F. Heatley, *Prog. Nucl. Magn. Reson. Spectrosc.*, 1979, **13**, 47–85.

3. ESTUDIO REOLÓGICO DE LAS SOLUCIONES DE QUITOSANO EN LÍQUIDOS IÓNICOS BASADOS EN IMIDAZOLIO

Los resultados de este capítulo corresponden al artículo científico titulado:

"Rheological study of chitosan solutions in imidazolium based ionic liquids"

Para envío a revisión a la revista Carbohydrate Polymers de la editorial Elsevier.

Rheological Study of Chitosan Solutions in Imidazolium Based Ionic Liquids

G. Santos-López,a E. Carvajal-Millán,a Y. L. López-Franco,a W. M. Argüelles-Monal,b M. T. Recillas-Mota,b J. Lizardi-Mendoza*a

a Centro de Investigación en Alimentación y Desarrollo, A.C., Laboratorio de Biopolímeros, P.O. Box 1735, Hermosillo, Sonora 83000, México., Fax: +52-662-289-2400; E-mail: jalim@ciad.mx

b Centro de Investigación en Alimentación y Desarrollo, A.C., Unidad Guaymas, P.O. Box 284, Guaymas, Sonora 85480, México., Fax: +52-662-221-6533

Abstract

Flow and viscosity parameters of chitosan solutions in imidazolium-based ionic liquids, 1-ethyl-3-methylimidazolium acetate, and 1-butyl-3-methylimidazolium acetate, were studied in a range of concentrations and temperatures. Both solvents and diluted chitosan solutions display a Newtonian type flow that becomes non-Newtonian above 1% of chitosan concentration. The Kreamer equation was used to determine the intrinsic viscosities. For both solvents, an increase in temperature causes a linear decrease of chitosan intrinsic viscosity. Using the obtained intrinsic viscosity values was possible to calculate the critical concentration of entanglement of Cs in each solvent. The effect of temperature on the viscosity of the solutions was studied by an Arrhenius type analysis that was used to determine the activation energies for both types of solutions. Such parameter was directly proportional to the concentration of chitosan.

Introduction

Ionic liquids (IL) are defined as liquids that are composed entirely of ions (Seddon, 1997). In a practical sense, IL are salts that remain melt below 100°C. These substances have become interesting to diverse green chemical processes due to their physicochemical properties; such as low vapor pressure, thermal stability, low melting point and tuneable solvation capacity (Murugesan and Linhardt, 2005). At the moment, the use of IL to dissolve several polysaccharides has been reported. Particularly, some imidazolium-based IL have been found suitable to dissolve typically resilient polysaccharides, as cellulose or chitin, even at relatively high concentrations (Swatloski et al., 2002; Wu et al., 2008; Xie et al., 2006). This has been key to the development of innovative methods to produce functional biopolymer materials and composites (Shen et al., 2015; Silva et al., 2017).

Chitosan is a linear polysaccharide formed by β(1-4) linked D glucosamine and N acetyl-D-glucosamine units (Fig. 10.A), where the former is present in higher proportion. The protonation of its amino groups allows the formation of solutions in the aqueous acid medium. Further details of the dissolution mechanism and the behavior of the polysaccharide molecule in aqueous acid solutions have been studied extensively (Rinaudo et al., 1999a, 1999b). Conversely, even when the dissolution of chitosan in imidazolium-based IL, such as 1-ethyl-3-methylimidazolium acetate (EMIMAc) and 1-butyl-3-methylimidazolium acetate (BMIMAc) (Fig. 10. B-C), has been reported (Chen et al., 2011; Xie et al., 2006) most of the studies were focused on obtain functional materials (Liu et al., 2012; Shen et al., 2015; Silva et al., 2011). Therefore, there are several aspects of the behavior of the chitosan molecules in IL solutions that have not been fully elucidated. To contribute to the knowledge of this interesting chitosan dissolution system the aim of this work is investigate the rheological properties of Cs in EMIMAc and BMIMAc at several concentrations and temperatures to determinate basic hydrodynamic parameters for each system.
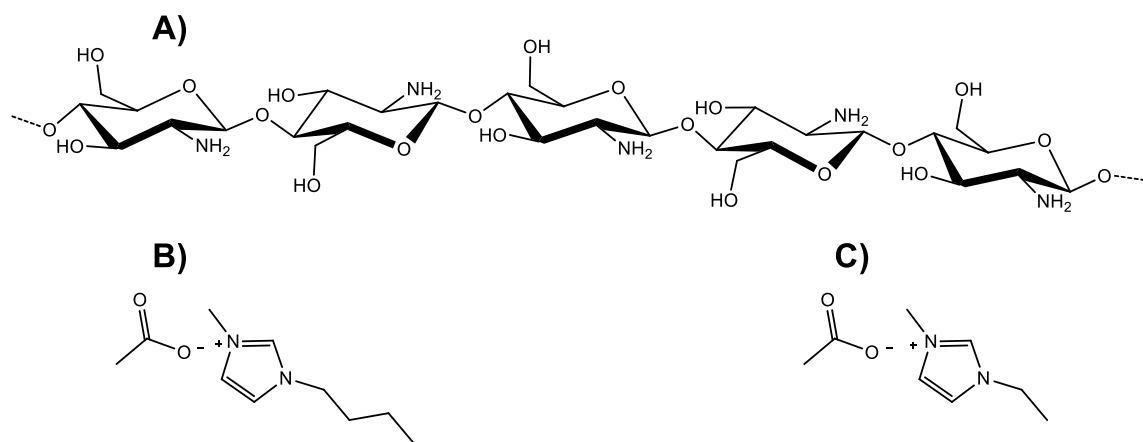
Figure 10. Schematic structure of chitosan (A), BMIMAc (B) and EMIMAc (C).

Methods

Materials. The ionic liquids, EMIMAc (90%) and BMIMAc (95%), were acquired at reagent grade (Sigma-Aldrich Co.). These solvents were stored in a desiccator at room temperature and used as arrived without further purification. *Pandalus borealis* shrimp chitosan (Primex, Batch No. TM 1961) was used for all experiments. The physicochemical characteristics of Cs are a degree of acetylation (DA) of 16.3%, determined by ^{13}C NMR; and weight average molecular mass (M_w) of 201.3x10^3 g/mol, measured by dynamic light scattering (Santos-López et al., 2017). Chitosan was purified before use as follow: First, a 0.5% (w/w) Cs solution in acetic acid was filtered successively through cellulose membranes of 8, 3, 1.2 and 0.8 µm. Then, the filtrate was neutralized (up to pH 8) with 10% NaOH. The precipitated Cs was washed thoroughly with an ethanol/water mixture. After a final water wash to remove the alcohol excess, the sample was freeze-dried and stored in a desiccator at room temperature until use.

Solutions preparation

Both solvents and chitosan were conditioned at 110 °C in vacuum for 24 hours before the preparation of the solutions. To dissolve the Cs metered quantities of IL were heated up to 110°C under nitrogen atmosphere. Then the polysaccharide was added in 0.2%

52

portions into the corresponding IL, waiting for complete dispersion, until getting 5.0% (w/w) mixtures. Such mixtures were magnetically agitated until clear solutions were achieved. The obtained solutions were used as stock to prepare the required concentration by dilution with the corresponding IL. All the tested solutions were prepared fresh before analysis and kept at 60°C in vacuum if necessary.

Rheology. Steady shear measurements were carried out in a Discovery HR-3 rheometer (TA Instruments) using a cone (60 mm, 2.0101°) to plate geometry and Peltier temperature control system. Shear rates were varied from 0.01 to 100 s^{-1} and temperatures from 0 to 50°C. Due to the highly hygroscopic nature of the IL, a DC200 silicone oil ring and a humidity trap cover with nitrogen gas displacement was used to prevent the moisture uptake of the solution during analysis.

Assuming a non-Newtonian behavior of the Cs solution in IL the "power law" relationship (Eq. 7) was used to calculate the viscosity (η).

$$\eta = k\dot{\gamma}^{n-1} \ (7)$$

Where '$\dot{\gamma}$' is the shear rate, 'k' is the consistency index, and 'n' is the flow index. The power law calculations were applied over flow curves to determinate the viscosity of the solutions using the built-in algorithms of the rheometer control software Trios™ v4.1.1.33073 (TA Instruments).

The intrinsic viscosity [η] was experimentally determined extrapolating to infinite dilution the tendency line of the viscosity of solutions in a low concentration range. For this, the Kraemer equation (Eq. 8) was applied.

$$\frac{\ln \eta_{rel}}{c} = [\eta] + k''[\eta]^2 c \ (8)$$

where 'η_{rel}' is viscosity of the solution relative to that of the solvent, and 'c' is the concentration in mL/g (taking into account the density of the respective IL and temperature) (Bogolitsyn et al., 2009; Hallett and Welton, 2011; Nazet et al., 2015; Tariq et al., 2009).

Results and discussion

Steady shear rheological experiments were used to investigate the flow of Cs solutions in EMIMAc and BMIMAc at several conditions. To illustrate the obtained results, the flow curves at 25°C of Cs solutions in EMIMAc and BMIMAc at different concentrations are included in Figure 2. It can be seen that pure EMIMAc has a lower viscosity than pure BMIMAc. Pure ILs exhibit a Newtonian plateau over three decades of shear rate (up to $\dot{\gamma} = 100 \; s^{-1}$). Similar patterns were also observed at other temperatures, this has been reported previously for EMIMAc (Gericke et al., 2009). In concordance with the characteristic behavior of polymer solutions the viscosity raises as the polymer concentration increases. The increment in the viscosity with concentration is more marked for EMIMAc solutions. The measured viscosity of such solutions reasonable compare quite well with those reported for solutions of microcrystalline cellulose and cellulose acetate in EMIMAc (Gericke et al., 2009; Rudaz and Budtova, 2013)

Newtonian flow behavior was also observed at low Cs concentrations (semi-dilute regime), up to 2% (w/w) in BMIMAc and 1% (w/w) in EMIMAc. For concentrations above these limits, the shear thinning effect is clearly observed, particularly for chitosan solutions in EMIMAc. For comparative purposes, the data from Fig. 11.A and 11.B have been superposed in Fig. 11.C, giving two master curves (reduced viscosity, η/η_0 ratio, as a function of the shear rate) for chitosan solution in both ILs at 25° C. This non-Newtonian effect has been explained as a consequence of the prevalence of intermolecular entanglements associated with the longest relaxation times over the transit time necessary for a pair of macromolecules to pervade the domain of each other as they shear (Ferry, 1980; Graessley, 1974). The fact that the shear thinning effect is less noticeable in the case of BMIM solutions (Fig. 11.C), is probably related with the longer aliphatic substituents of the BMIM counter ions diminishing the terminal relaxation times of topological entanglements as compared with the shear flow. As it will become apparent later in this work, these limiting polymer concentration values for

54

the Newtonian flow seem to coincide with the critical concentration denoting the boundaries of the semi-dilute regime.
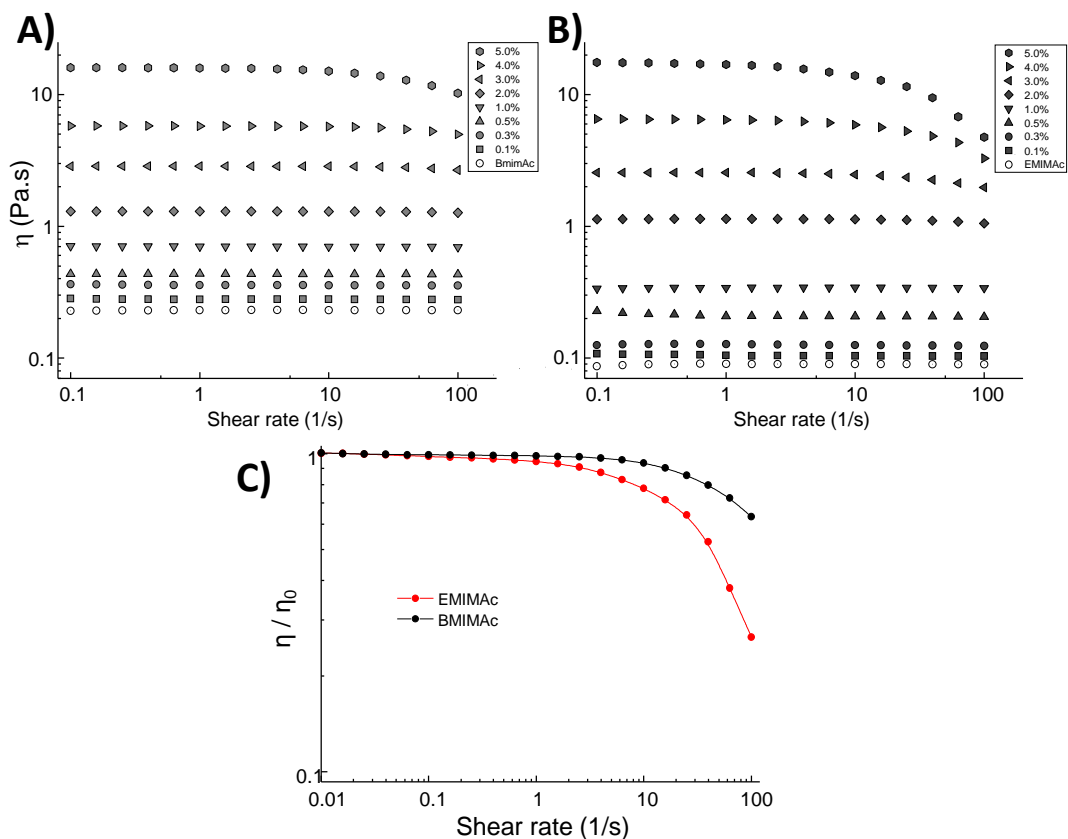
Figure 11. Flow curves at 25° C of Cs solutions in BMIMAc (A) or EMIMAc (B) and the superimposed master curves of the relative viscosity of both type of solutions (C).

The ηrel of Cs solutions in BMIMAc and EMIMAc at different temperatures and concentrations are presented in Figure 12. In both systems the relative viscosities increase nonlinearly above a concentration of 1%, a similar behavior has been observed for Cs in dilute solution with acid (Argüelles-Monal et al., 1998) and with different random coil polysaccharides dissolved in aqueous solutions (Morris et al., 1981).

.
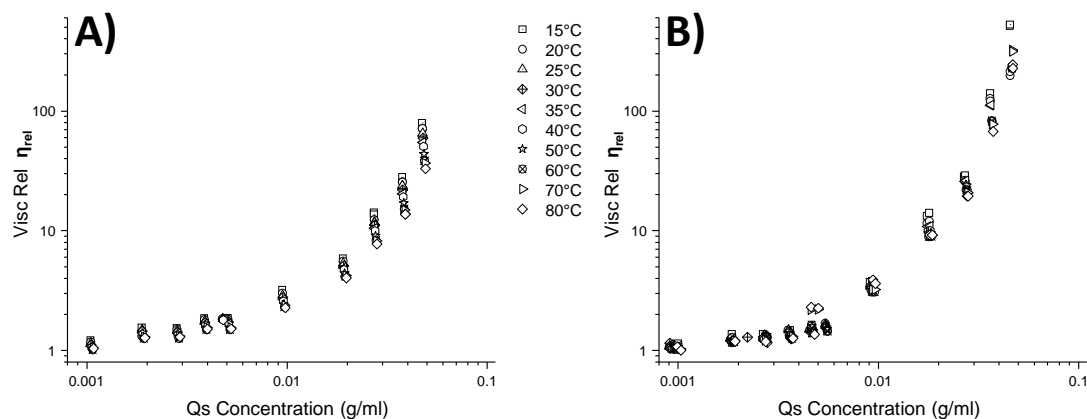
Figure 12. Relation of the relative viscosity of Cs solutions with the concentration at different temperatures. CsBMIMAc (A), CsEMIMAc (B).

The intrinsic viscosity ([η]) of chitosan in EMIMAc and BMIMAc was determined using the Kraemer equation (Eq. 8). The [η] of Cs in BMIMAc is considerably higher than in EMIMAc (Figure 13.). Considering that [η] could be used as a convenient index of the size (hydrodynamic volume) of the polymer in solution (Morris et al., 1981), the Cs molecules appear to be more extended in BMIMAc. However, the formation of molecular aggregates in such solution could not be ruled out completely. On the other hand, the apparent size of Cs in IL is lower than in aqueous acid solutions (Argüelles-Monal et al., 1998), where the electrostatic repulsion between adjacent protonated amino groups force the Cs molecules to adopt more extended configurations

In Fig. 13. could be also appreciated that [η] decreases when the temperature is increased. The dependence of the [η] with temperature could be characterized using an Arrhenius type plot (Fig. 13.B). The rise of molecular dynamic with temperature with the reduction of the observed [η] values could lead to being interpreted as an apparent reduction of the hydrodynamic volume of Cs in IL solutions.

The obtained intrinsic viscosities were used to build a master plot, ηrel in function of the coil overlap parameter (c[η]), for both type of Cs solutions at the whole range of temperatures studied (Figure 14.). From this construct is possible to estimate the critical concentration of entanglement (c*). At low degrees of space occupancy, a dependence of ηrel ~ c[η]1.22 for CsEMIMAc indicates a c* just above 0.5% (w/w). On the other hand, for the system CsBMIMAc the dependence of ηrel ~ c[η]2.0 correspond to c* above 1.0% (w/w).

56
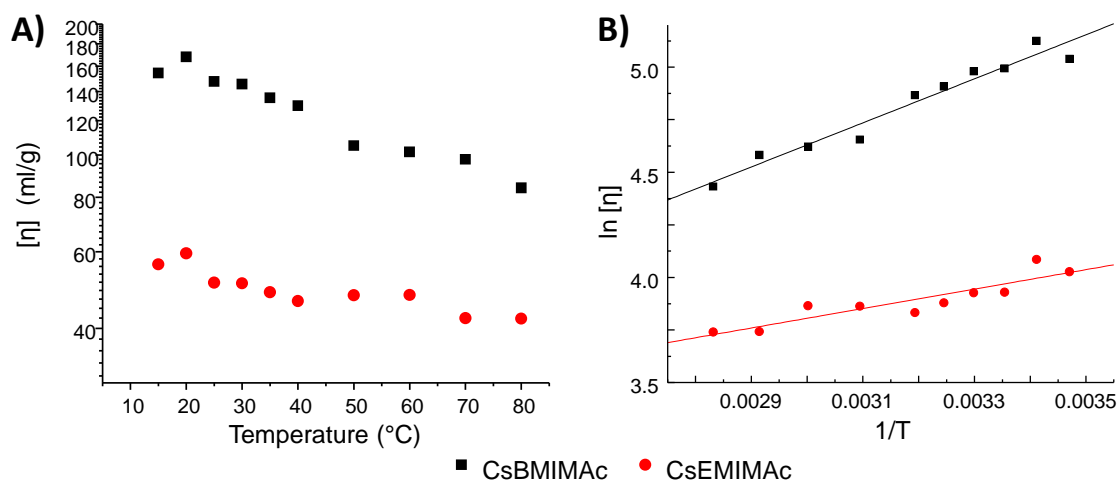
Figure 13. The intrinsic viscosity of Cs solutions in ionic liquids (A) and Arrhenius type plot showing the effect of the temperature on this parameter (B).
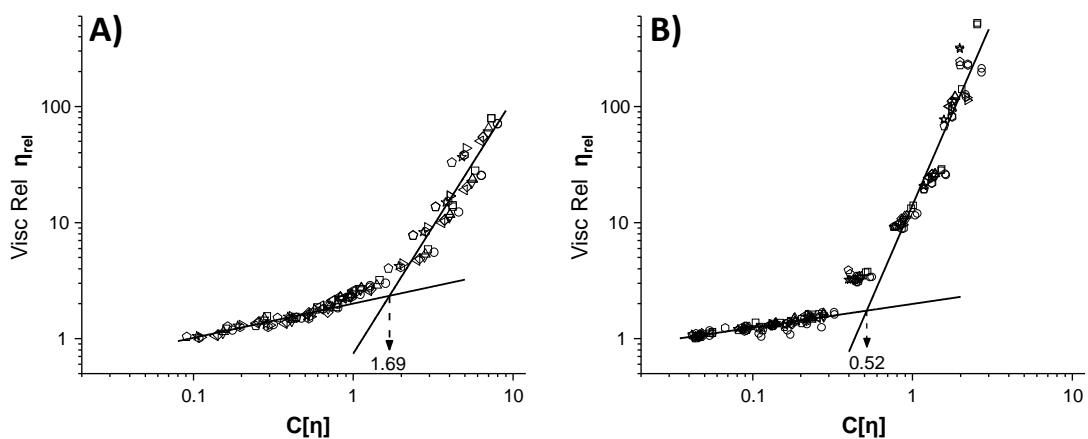
Figure 14. Master plots of variation of ηrel with space occupancy parameter c[η] for chitosan solutions in BMIMAc (A) and EMIMAc (B).

Conventional Arrhenius type analysis was used to estimate the effect of the temperature on the viscosity. There is a linear dependence of the 'ln η' with the inverse of the temperature for all concentrations of both Cs solutions tested. From these plots, it was possible to calculate the activation energy (Ea) parameters for each Cs concentration in EMIMAc and BMIMAc. The Ea of each type of solution increases linearly with Cs concentration (Figure 15.). The values for CsBMIMAc are slightly higher than those for

CsEMIMAc; however the slope for the EMIMAc solution [354 KJ•mol•(mg/ml)-1] is higher than for the BMIMAc solution [(181 KJ•mol•(mg/ml)-1]. These observations could be related to the different viscosity of the solvents and the apparent hydrodynamic volume of chitosan in each IL (Gericke et al., 2009; Sescousse et al., 2010).
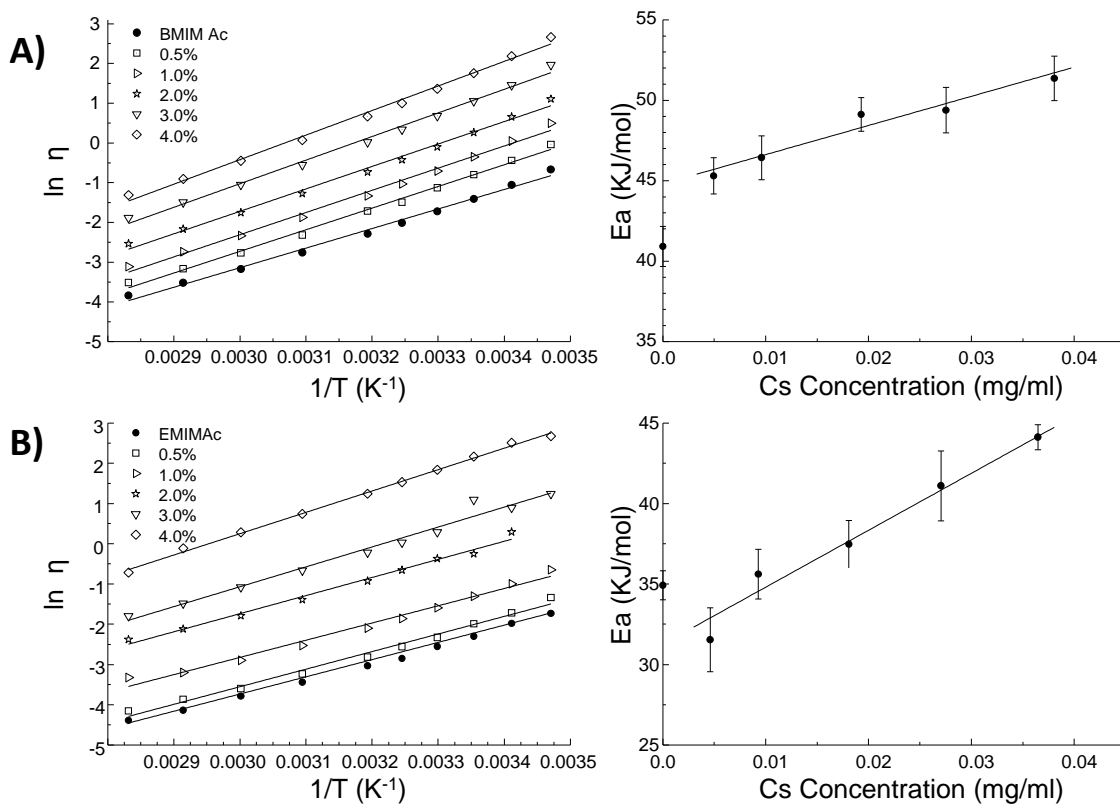
Figure 15. Arrhenius type analysis of viscosity of chitosan solutions in BMIMAc (A) and EMIMAc (B).

Conclusions

The effect of the temperature and polymer concentration on the flow and viscosity parameters of chitosan in two imidazolium-based ionic liquids, EMIMAc and BMIMAc, was studied. Both solutions behave as Newtonian fluids at concentrations below 1%, above that concentration become pseudoplastic fluids. The intrinsic viscosity of chitosan was determined using the Kraemer approach and is reported for the first time for solutions in these IL. The $[\eta]$ was lower for Cs in EMIMAc than in BMIMAc; furthermore, both intrinsic viscosities are lower than previously reported values for Cs in aqueous acid solutions. This could indicate that chitosan has smaller hydrodynamic volume adopting a relatively compact conformation in these imidazolium-based IL. Additionally, it was observed the inverse dependence of the $[\eta]$ with the temperature that could be adjusted to an Arrhenius type fitting. The critical concentration of entanglement (c*) was also estimated for both types of solutions. This information is useful to produce diverse materials as gels or nanoparticles. The effect of the temperature on the viscosity of the obtained solutions was further studied. The activation energies of both types of solutions at various chitosan concentrations were determined. The Ea varies linearly with the Cs concentration, but with higher slope in EMIMAc solutions.

References

Argüelles-Monal, W., Goycoolea, F.M., Peniche, C., and Higuera-Ciapara, I. (1998). Rheological study of the chitosan/glutaraldehyde chemical gel system. Polym. Gels Netw. 6, 429–440.

Bogolitsyn, K.G., Skrebets, T.E., and Makhova, T.A. (2009). Physicochemical properties of 1-butyl-3-methylimidazolium acetate. Russ. J. Gen. Chem. 79, 125–128.

Chen, Q., Xu, A., Li, Z., Wang, J., and Zhang, S. (2011). Influence of anionic structure on the dissolution of chitosan in 1-butyl-3-methylimidazolium-based ionic liquids. Green Chem. 13, 3446–3452.

Ferry, J.D. (1980). Viscoelastic Properties of Polymers (John Wiley & Sons).

Gericke, M., Schlufter, K., Liebert, T., Heinze, T., and Budtova, T. (2009). Rheological Properties of Cellulose/Ionic Liquid Solutions: From Dilute to Concentrated States. Biomacromolecules 10, 1188–1194.

Graessley, W.W. (1974). The entanglement concept in polymer rheology. In The Entanglement Concept in Polymer Rheology, (Springer Berlin Heidelberg), pp. 1–179.

Hallett, J.P., and Welton, T. (2011). Room-Temperature Ionic Liquids: Solvents for Synthesis and Catalysis. 2. Chem. Rev. 111, 3508–3576.

Liu, Z., Wang, H., Liu, C., Jiang, Y., Yu, G., Mu, X., and Wang, X. (2012). Magnetic cellulose–chitosan hydrogels prepared from ionic liquids as reusable adsorbent for removal of heavy metal ions. Chem. Commun. 48, 7350–7352.

Morris, E.R., Cutler, A.N., Ross-Murphy, S.B., Rees, D.A., and Price, J. (1981). Concentration and shear rate dependence of viscosity in random coil polysaccharide solutions. Carbohydr. Polym. 1, 5–21.

Murugesan, S., and Linhardt, R.J. (2005). Ionic Liquids in Carbohydrate Chemistry - Current Trends and Future Directions. Curr. Org. Synth. 2, 437–451.

Nazet, A., Sokolov, S., Sonnleitner, T., Makino, T., Kanakubo, M., and Buchner, R. (2015). Densities, Viscosities, and Conductivities of the Imidazolium Ionic Liquids [Emim][Ac], [Emim][FAP], [Bmim][BETI], [Bmim][FSI], [Hmim][TFSI], and [Omim][TFSI]. J. Chem. Eng. Data 60, 2400–2411.

Rinaudo, M., Pavlov, G., and Desbrières, J. (1999a). Influence of acetic acid concentration on the solubilization of chitosan. Polymer 40, 7029–7032.

Rinaudo, M., Pavlov, G., and Desbrières, J. (1999b). Solubilization of Chitosan in Strong Acid Medium. Int. J. Polym. Anal. Charact. 5, 267–276.

Rudaz, C., and Budtova, T. (2013). Rheological and hydrodynamic properties of cellulose acetate/ionic liquid solutions. Carbohydr. Polym. 92, 1966–1971.

Santos-López, G., Argüelles-Monal, W., Carvajal-Millan, E., López-Franco, Y.L., Recillas-Mota, M.T., and Lizardi-Mendoza, J. (2017). Aerogels from Chitosan Solutions in Ionic Liquids. Polymers 9, 722.

Seddon, K.R. (1997). Ionic Liquids for Clean Technology. J. Chem. Technol. Biotechnol. 68, 351–356.

Sescousse, R., Le, K.A., Ries, M.E., and Budtova, T. (2010). Viscosity of Cellulose−Imidazolium-Based Ionic Liquid Solutions. J. Phys. Chem. B 114, 7222–7228.

Shen, X., Shamshina, J.L., Berton, P., Gurau, G., and Rogers, R.D. (2015). Hydrogels based on cellulose and chitin: fabrication, properties, and applications. Green Chem. 18, 53–75.

Silva, S.S., Duarte, A.R.C., Carvalho, A.P., Mano, J.F., and Reis, R.L. (2011). Green processing of porous chitin structures for biomedical applications combining ionic liquids and supercritical fluid technology. Acta Biomater. 7, 1166–1172.

Silva, S.S., Mano, J.F., and Reis, R.L. (2017). Ionic liquids in the processing and chemical modification of chitin and chitosan for biomedical applications. Green Chem. 19, 1208–1220.

Swatloski, R.P., Spear, S.K., Holbrey, J.D., and Rogers, R.D. (2002). Dissolution of Cellulose with Ionic Liquids. J. Am. Chem. Soc. 124, 4974–4975.

Tariq, M., Forte, P.A.S., Gomes, M.F.C., Lopes, J.N.C., and Rebelo, L.P.N. (2009). Densities and refractive indices of imidazolium- and phosphonium-based ionic liquids: Effect of temperature, alkyl chain length, and anion. J. Chem. Thermodyn. 41, 790–798.

Wu, Y., Sasaki, T., Irie, S., and Sakurai, K. (2008). A novel biomass-ionic liquid platform for the utilization of native chitin. Polymer 49, 2321–2327.

Xie, H., Zhang, S., and Li, S. (2006). Chitin and chitosan dissolved in ionic liquids as reversible sorbents of CO2. Green Chem. 8, 630–633.

4. AEROGELES DE SOLUCIONES DE QUITOSANO EN LÍQUIDOS IÓNICOS

Este capítulo comprende el artículo científico:

"Aerogels from chitosan solutions in ionic liquids"

Publicado en la revista Polymers, de la editorial MDPI, en el 2017, volumen 9, número 12, página 722; DOI: 10.3390/polym9120722.

Article

Aerogels from Chitosan Solutions in Ionic Liquids

Gonzalo Santos-López [1], Waldo Argüelles-Monal [2] iD, Elizabeth Carvajal-Millan [1], Yolanda L. López-Franco [1] iD, Maricarmen T. Recillas-Mota [2] and Jaime Lizardi-Mendoza [1],* iD

[1] Grupo de Investigación en Biopolímeros—CTAOA. Centro de Investigación en Alimentación y Desarrollo, A.C., Hermosillo, Sonora 83304, Mexico; gonzalosantos@estudiantes.ciad.mx (G.S.-L.); ecarvajal@ciad.mx (E.C.-M.); lopezf@ciad.mx (Y.L.L.-F.)

[2] Polímeros Naturales. Centro de Investigación en Alimentación y Desarrollo, A.C., Unidad Guaymas, Guaymas, Sonora 85480, Mexico; waldo@ciad.mx (W.A.-M.); mrecillas@ciad.mx (M.T.R.-M.)

* Correspondence: jalim@ciad.mx; Tel.: +52-662-289-2400

Abstract: Chitosan aerogels conjugates the characteristics of nanostructured porous materials, i.e., extended specific surface area and nano scale porosity, with the remarkable functional properties of chitosan. Aerogels were obtained from solutions of chitosan in ionic liquids (ILs), 1-butyl-3-methylimidazolium acetate (BMIMAc), and 1-ethyl-3-methyl-imidazolium acetate (EMIMAc), in order to observe the effect of the solvent in the structural characteristics of this type of materials. The process of elaboration of aerogels comprised the formation of physical gels through anti-solvent vapor diffusion, liquid phase exchange, and supercritical CO_2 drying. The aerogels maintained the chemical identity of chitosan according to Fourier transform infrared spectrophotometer (FT-IR) spectroscopy, indicating the presence of their characteristic functional groups. The internal structure of the obtained aerogels appears as porous aggregated networks in microscopy images. The obtained materials have specific surface areas over 350 m^2/g and can be considered mesoporous. According to swelling experiments, the chitosan aerogels could absorb between three and six times their weight of water. However, the swelling and diffusion coefficient decreased at higher temperatures. The structural characteristics of chitosan aerogels that are obtained from ionic liquids are distinctive and could be related to solvation dynamic at the initial state.

Keywords: aerogels; chitosan; ionic liquids; ionogels

1. Introduction

Chitosan (Cs) is a natural linear polysaccharide generated from the deacetylation of chitin and is composed of β-(1-4)-D-glucosamine units and β-(1-4)-*N*-acetyl-glucosamine distributed along the polymeric chain. The physicochemical characteristics and functional properties of Cs, such as its polycationic character, biocompatibility, low toxicity, and structural capacity, make it a polysaccharide of interest in different fields. The mechanical and structural properties of chitosan allow for different types of materials to be obtained from chitosan solutions, e.g., nanostructured porous materials. Aerogels are a specific type of nanostructured porous material that are characterized by mesopores (pore diameter between 2 and 50 nm) and large surface areas. Obtaining aerogels of chitosan could improve the availability of the functional groups of chitosan [1]. Together, the aerogel characteristics with the functional properties of chitosan, potentially provides materials with multiple applications, e.g., adsorption, transport, and controlled release of bioactive molecules, toxics, and pollutants removers, among others.

Ionic liquids (IL) are an alternative medium for chitosan dissolution. When compared to the traditional aqueous acid solvents used to dissolve Cs, IL have different physicochemical characteristics because they consist of only ions and water is not needed to dissolve chitosan. Most of the

studies of chitosan with IL have been focused on the formation of solutions. Imidazolium based IL, as 1-butyl-3-methylimidazolium acetate (BMIMAc), and 1-ethyl-3-methyl-imidazolium acetate (EMIMAc), have been highlighted because they are able to dissolve chitosan at high concentrations (up to 10% *w/w*). Other reports have focused on forming materials from chitosan solutions in IL e.g., fibers, blends, films, membranes, hydrogels, and ionogels [2–12]. Aerogels from chitin with BMIMAc solutions has been reported [13], but the information about chitosan ionogels and aerogels from IL solutions is limited.

Supercritical CO_2 drying, unlike other types of drying, keeps most of the internal structure formed at gelation because the effects of surface tension on the three-dimensional macromolecular network are minimized. Therefore, chitosan aerogels that are generated from solutions of Cs in IL (BMIMAc and EMIMAc) were produced in order to study the physicochemical characteristics of these novel materials. Concurrently, observations on the structural features of the aerogels could be related to the network formation and molecular conformation of chitosan in ionic liquids at the physical gelling process.

2. Materials and Methods

2.1. Materials

Shrimp shells (*Pandalus borealis*) Cs was acquired from Primex (batch No. TM 1961, Siglufjörður, Iceland). The degree of acetylation (DA) of Cs was 16.3%, as determined by solid-state cross-polarization magic angle spinning ^{13}C nuclear magnetic resonance spectroscopy (CP/MAS ^{13}C-NMR) performed in a Bruker Avance TM 400WB (Bruker Biospin, Wissembourg, France, 9.4 Tesla, 1 ms contact time, 2000 scans) [14,15]. The weight average molecular weight (M_w) of Cs was 2.01×10^5 g/mol, determined by static light scattering, as described previously [16]. Chitosan was purified, as described by Rinaudo et al. (1999), before use it [17]. Commercial grade IL, BMIMAc and EMIMAc (BASF, Steinheim, Germany), were used as received just prior each use they were stored in desiccator and kept at 105° C for 24 h in vacuum to minimize moisture. High grade supercritical drying liquid CO_2 (99.99% purity) was supplied by Infra (Hermosillo, México). All of the compounds and solvents that were used were reagent grade acquired from recognized commercial chemical distributors. The water used for the experiments was deionized type I (resistivity of 18.2 MΩ·cm at 25 °C) unless stated otherwise.

2.2. Solutions of Chitosan in Ionic Liquids

The moisture-free IL was added into a round-bottom flask with a sufficient amount of chitosan to obtain a 2% (*w/w*) concentration. This solution was heated in an oil bath at 105 °C under magnetic stirring at least 6 hours under a nitrogen atmosphere. Upon complete Cs dissolution it was stored in a desiccator at room temperature until use. Two types of solutions were obtained: Cs in EMIMAc (CsEMIM) and Cs in BMIMAc (CsBMIM).

2.3. Formation of Ionogels

The physical gels were formed using approximately 0.1 g of the Cs-IL solution that was casted in cylindrical containers (0.4 cm diameter), with the bottom being covered with plastic paraffin film. Gelation was induced by vapor diffusion of an antisolvent, such as ethanol or water, in a closed chamber [18]. The gels were recovered after 48 h and were transferred to a 70% ethanol aqueous mixture. These gels that contain IL as liquid phase confined within a polymer matrix are defined as ionogels [19].

2.4. Formation of Aerogels

The ionogels were thoroughly rinsed with aqueous ethanol (70%) until the IL was completely removed. The presence of IL in the rinsing media was monitored with UV/VIS spectroscopy, scanning between 190 to 300 nm using the ethanol-water mixture as reference. Afterwards, the liquid phase

65

was replaced with acetone, which has higher miscibility with supercritical CO_2. For this, the gels were repeatedly rinsed with a gradient of acetone-water mixtures that ended with two rinses with pure acetone. The acetogels (gels containing acetone as fluid phase) were dried with supercritical CO_2 (>32 °C and 73 atm) in a pressurized reactor. At the end of the process, the dried aerogels were stored in a desiccator at room temperature.

2.5. Characterization of Aerogels

2.5.1. Chemical Identity

The chemical composition of the samples was determined analyzing the characteristic bands in the infrared spectrum obtained by a Fourier transform infrared spectrophotometer (FT-IR, Thermo Scientific, Nicolet iS-50, Madison, WI, USA), using the attenuated total reflection (ATR) mode. All of the measurements were performed at room temperature collecting 32 scans at $4 \, \text{cm}^{-1}$ resolution.

2.5.2. Structural Analysis

The surface area, pore volume, and nitrogen adsorption and desorption isotherms of the aerogels were determined with the surface area analyzer Nova 2200e (Quantachrome Instruments, Boynton Beach, FL, USA), and analysis of the data with the software NovaWin version 11.02 (Quantachrome Instruments, Boynton Beach, FL, USA). The morphological characteristics of the aerogels were thoroughly observed by field emission scanning electron microscopy (Hitachi SU8000, Tokyo, Japan). The images were obtained using an accelerating voltage of 1.0 KeV.

2.5.3. Degree of Swelling

The swelling capacity of the aerogels at equilibrium was determined from their immersion in water at different temperatures (20, 25, 30, and 40 °C). The weight gain of the samples was periodically monitored by removing the excess of water with filter paper. Equation (1) was used to estimate the degree of swelling (W), as follows:

$$W = \frac{P - P_0}{P_0} = \frac{P}{P_0} - 1 \tag{1}$$

where P_0 is the weight of the dry aerogel and P is the weight of the aerogel in the wet state [20].

3. Results and Discussion

The vapor diffusion of a non-solvent agent was useful to produce ionogels from Cs solutions in IL. By this way, it was possible to obtain three different types of physical chitosan ionogels (Table 1). Using ethanol as non-solvent agent gels were obtained from both Cs-IL solutions. These gels were clear, rigid, and brittle; the only noticeable difference among them was the color tone, darker yellow for the gels from CsBMIM. It has been indicated that the main effect of IL on polysaccharides is to disrupt the hydrogen bonds and promoting their dissolution. Low molecular weight alcohols are miscible with imidazolium based ionic liquids [21], but chitosan does not dissolve in alcohols. Therefore, when ethanol diffuses into a Cs-IL solution, the solvation effect of the ionic liquid over chitosan decreases, favoring the interactions between chitosan chains and subsequently leading to the generation of a gel. Conversely, water vapor was only useful to produce gels from the CsEMIM solution. It has been noticed that BMIMAc has a lower affinity for water than EMIMAc [22], this could be related to lower diffusion rates that do not decrease its chitosan solvation capacity in preventing the gel formation. It should be taken in account that chitosan do not dissolve in water, but it is hygroscopic. As result, the obtained gels from water diffusion were weak and difficult to manipulate without compromising their integrity. Hence, subsequent procedures and analysis were performed using only ionogels that are produced by ethanol treatment.

Table 1. Outcome of the treatment of Cs-IL solutions with non-solvent agents vapor diffusion.

Cs-IL Solution	Non-Solvent Agent	
	Water	Ethanol
CsEMIM	Ionogel (soft)	Ionogel (CsE)
CsBMIM	dilution	Ionogel (CsB)

When the ionogels were rinsed with an ethanol-water mixture they became more translucent, reducing their yellow color (Figure 1). The continuous rinsing of the gels gradually eliminated the ionic liquid from inside the gels. The ethanol concentration that was used allowed for keeping the ionogels volume without causing drastic swelling or shrinkage. In the subsequent fluid phase replacement with acetone, the CsE ionogels decrease 25% their volume, and in the case of CsB, the reduction was 42%. Apparently, the chitosan chains underwent rearrangement within the formed network to a more stable configuration as a result of the interaction with acetone [23].
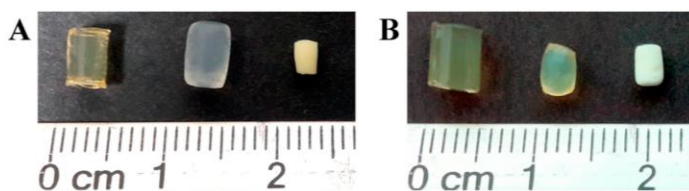
Figure 1. Materials formed from the Cs-IL solutions: (**A**) CsE and (**B**) CsB. From left to right: ionogel, acetogel and aerogel.

The obtained aerogels were rigid and brittle cylinders with opaque white color (Figure 1). The volume reduction when compared to the starting ionogels was of 73% for CsE and 82% for CsB. This behavior is similar to that reported for aerogels obtained from chitosan and κ-carrageenan [24]. Such volume reduction has been associated with the rearrangements of chitosan chains due to their lower affinity for acetone. This molecular movement does not cease until all of the acetone has been removed, even when the supercritical CO_2 drying reduce the effects of surface tension in the material [25].

3.1. Characterization of Chitosan Aerogels

The infrared spectra (2000–500 cm^{-1}) of chitosan and the obtained aerogels are shown in Figure 2. The main characteristic bands of chitosan are also observed in the aerogels spectra. At 1652 cm^{-1} is observed the stretching vibration band of the C=O bond that is associated to the amide I; the amide II –NH_2 deformation is related to the band at 1580 cm^{-1}; the band at 1424 cm^{-1} is associated to the CH_2 bending; at 1380 cm^{-1}, the symmetrical vibration deformation of the CH_3 group is observed; the band at 1318 cm^{-1} is associated to the amide III; the antisymmetric tension mode of the COC bridge is observed at 1150 cm^{-1}; finally, the fingerprint zone, between 1075 and 1026 cm^{-1}, is characteristic of the polysaccharides [26,27]. There is no evident modification on the spectra that indicate chemical changes in the chitosan as result of the gel formation or the drying process. Furthermore, there are not absorbance bands that could be related to the presence of residual IL in the aerogels.

67
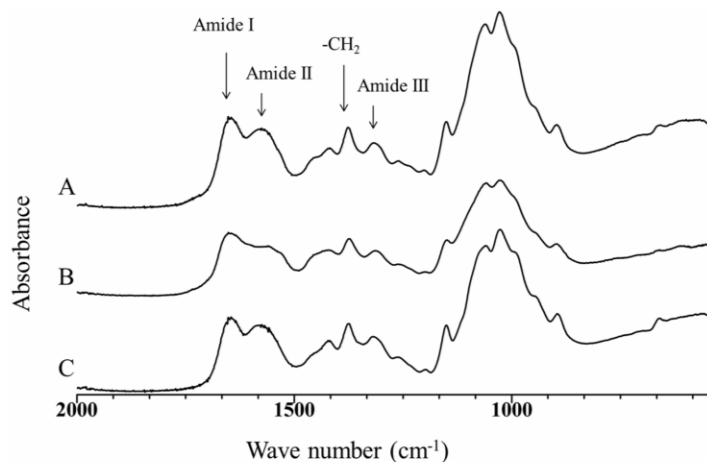
Figure 2. Fourier transform infrared spectrophotometer (FT-IR) spectra of (**A**) CsE aerogel; (**B**) CsB aerogel and (**C**) chitosan.

The N_2 adsorption and desorption isotherms of both types of aerogels are classified as type IV according to the IUPAC conventions (Figure 3). The observed hysteresis of N_2 desorption at high relative pressures is indicative of a mesoporous dry material [28]. The specific surface area (S_{BET}) and pore volume that are calculated from the adsorption and desorption isotherms are included in Table 2. The specific surface areas of the aerogels are in the higher rank when compared with other pure polysaccharide aerogels [24,29,30]. The pore size obtained was within the range of mesopores, which is characteristic of aerogels.
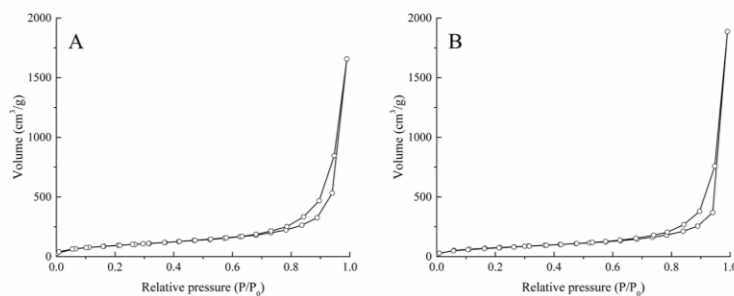
Figure 3. N_2 adsorption and desorption BET isotherms of (**A**) CsE and (**B**) CsB aerogels.

Table 2. Specific surface area (S_{BET}), pore volume (V_p) and pore diameter (D_p) of the CsE and CsB aerogels.

Parameters	CsE	CsB
S_{BET} (m^2/g)	358 ± 79	478 ± 264
V_p (cm^3/g)	0.0733 ± 0.016	0.236 ± 0.083
D_p (nm)	31.0 ± 1.4	46.0 ± 3.6

The scanning electron microscopy (SEM) images of the aerogels are shown in Figures 4 and 5. Both of the aerogels appear as uniform materials with some imperfections, which could be caused by fracture events. At the highest magnification available ($\times 10,000$), the internal structure of the aerogels looks as aggregated clumps forming a compact network with heterogeneous pores. The appearance of

the pores is consistent with the mesoporous characteristics of the aerogels. The main difference between both types of aerogels is that the internal structure of CsB appears to be denser. The internal structure of the aerogels produced from ionogels is different to previously reported chitosan aerogels [24,29]. These differences could be related to the solvent-polymer interaction. Electrostatic repulsions dominate in the aqueous acid chitosan solutions. In such conditions, the polysaccharide molecules adopt an extended hydrodynamic volume conformation [17]. Conversely, these repulsive forces are absent in Cs-IL solutions; thus, the chitosan molecules have relatively smaller dimensions, generating more compact structures in their aerogels.
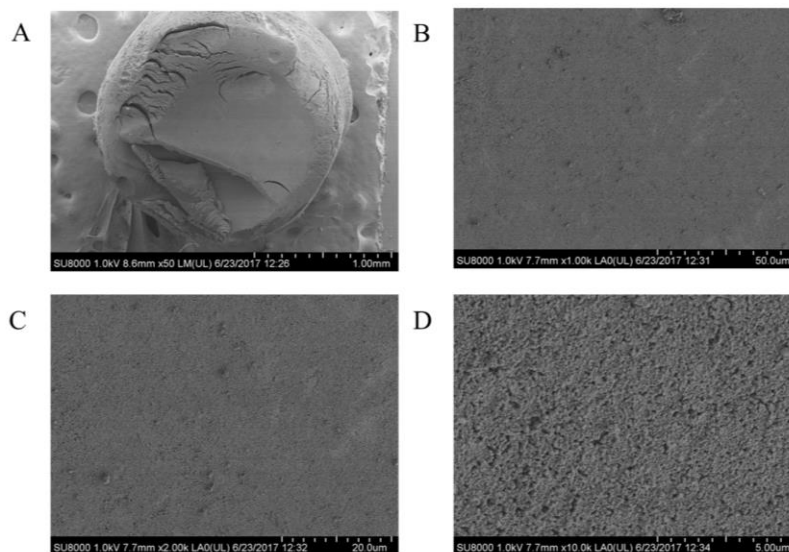
Figure 4. SEM images of the CsE aerogels (**A**) 50×; (**B**) 1000×; (**C**) 2000×; and, (**D**) 10,000× magnification.
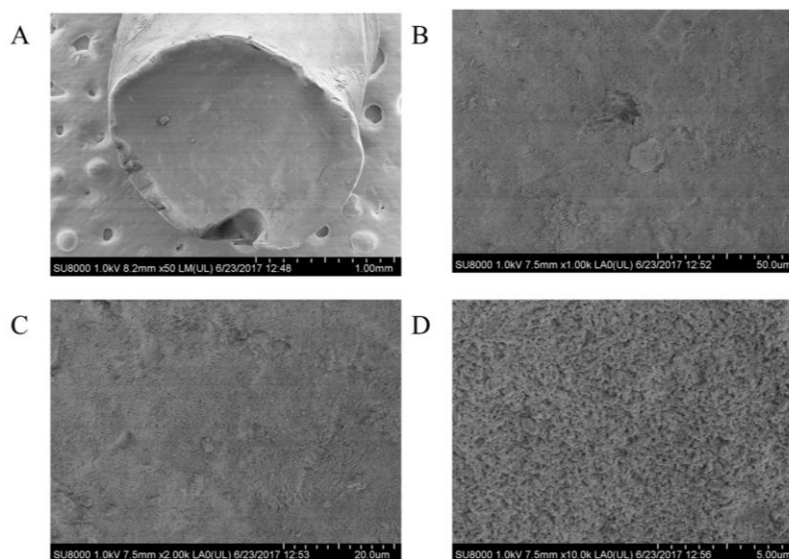
Figure 5. SEM images of the CsB aerogels. (**A**) 50×; (**B**) 1000×; (**C**) 2000×; and, (**D**) 10,000× magnification.

69

3.2. Diffusion Properties of Aerogels

The physical characteristics of aerogels, such as their large surface area and mesoporosity, endow these materials with a large capacity to adsorb certain compounds. The diffusion properties are key to evaluating the performance of these materials for important applications in pharmacy and biotechnology, among others. For this purpose, dried aerogels that are obtained from chitosan solutions in EMIMAc and BMIMAc, as described previously, were swollen in water at different temperatures between 20 and 40 °C and their kinetics was followed. In Figures 6 and 7, the experimental data is presented.

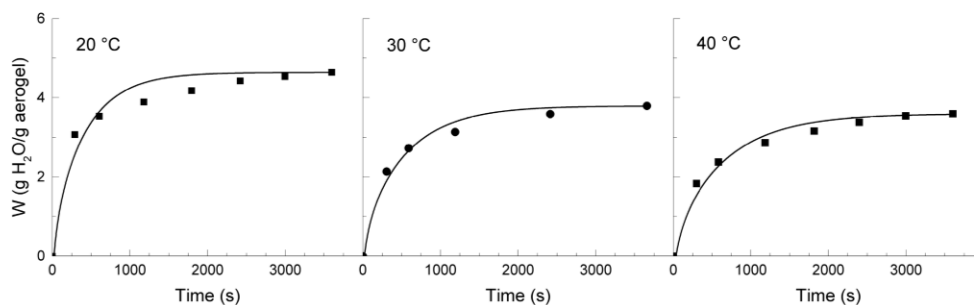**Figure 6.** Swelling curves of the CsE aerogels in water at different temperatures (20, 30, and 40 °C). Experimental data (points) and adjustment (lines) with Equation (2) are included.
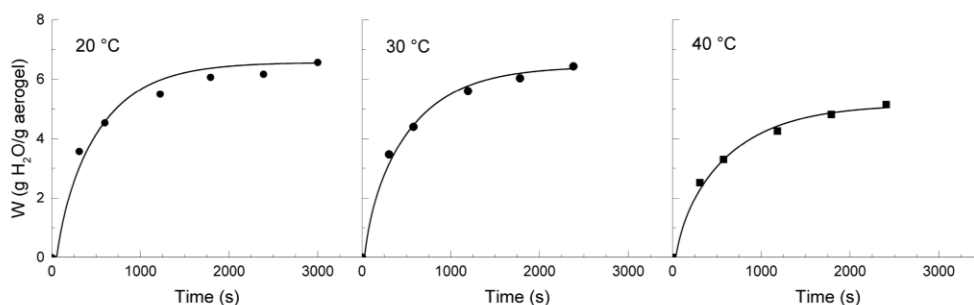
Figure 7. Swelling curves of the CsB aerogels in water at different temperatures (20, 30, and 40 °C). Experimental data (points) and adjustment (lines) with Equation (2) are included.

The CsE aerogels absorbed between three and four times their weight and exhibited a decreasing swelling capacity with an increasing temperature. In contrast, the CsB aerogels showed a greater capacity of absorption (between five and six times their weight), and the effect of temperature on the swelling capacity seems to be less marked. When compared with the aerogels of chitosan that was obtained from aqueous acid solutions, the aerogels from chitosan in IL showed higher W_∞. Previous studies with chitosan or chitosan-polyelectrolyte complex matrices that were prepared from aqueous media have shown a similar tendency to decrease the swelling capacity with temperature [20,31].

The Fick's law equation resolved for diffusion through a circular cylinder of radius r, keeping the diffusant concentration constant, becomes [32]:

$$\frac{W}{W_\infty} = 1 - \sum_{n=1}^{\infty} \frac{4}{r^2 \alpha_n^2} \exp\left(-D\alpha_n^2 t\right),$$

(2)

in which W is the swelling degree at time t, and W_∞ is the corresponding quantity at equilibrium, α_n^2 are the n first positive roots of the Bessel function of the first-kind, and D is the diffusion coefficient.

Equation (3) was solved for the first 15 terms of the summation and the diffusion coefficients that were adjusted through a non-linear least square fitting process. In all situations, satisfactory adjustments were obtained from Equation (2), as could be appreciated from the curves that are traced in Figures 6 and 7. The estimated values of D are summarized in Table 3. The diffusion coefficients are similar for both types of aerogels and compare to those that are reported for swelling of other polymeric materials [20,33]. It should be remarked, however, the unusual trend that exhibits the diffusion coefficient, decreasing with the increase in temperature.

Table 3. Values of the degree of swelling, diffusion coefficient, second-order kinetic constant and the release exponent of CsE and CsB aerogels of swelled in water at different temperatures.

T (°C)	CsE				CsB			
	W_∞ (g H_2O/g gel)	$D \times 10^{10}$ (m^2/s) [a]	$k \times 10^4$ (s^{-1}) [b]	n [c]	W_∞ (g H_2O/g gel)	$D \times 10^{10}$ (m^2/s) [a]	$k \times 10^4$ (s^{-1}) [b]	n [c]
20	4.64	3.99	3.011	0.16	6.56	3.36	1.111	0.26
25	3.96	3.55	3.426	0.20	5.22	3.32	1.367	0.31
30	3.79	3.01	3.464	0.23	6.43	3.09	1.703	0.35
40	3.59	2.54	4.481	0.29	5.15	2.68	2.738	0.37

[a] Evaluated according to Equation (2), [b] Evaluated according to Equations (8) and (10), [c] Dimensionless release exponent from the power law relation.

It is well known that diffusion coefficients have a dependence on temperature that is similar to the Arrhenius equation:

$$D = D_0 exp\left(-\frac{E_D}{RT}\right) \tag{3}$$

where E_D is the apparent activation energy for the diffusion process. For both aerogels, the expected linear dependence was obtained, but as a result of the inverse tendency that is shown by the diffusion coefficients with the temperature (Table 3), negative activation energy values were obtained. From a physical point of view, this fact indicates that there is another process competing with the diffusion, giving rise to negative values of this parameter. On the other hand, an analysis of the swelling values as a function of time, for each material at each temperature, according to the power law relation $W = kt^n$, allowed for finding the values of the release exponent, n, which are shown in the Table 3. Here, again, values are obtained that have no physical sense (for cylinders, n should be between 0.46 and 1) [34]. As seen above, both of the aerogels have a porous structure, with pore sizes ranging between 15 and 23 nm. According to these morphological characteristics, it should be expected that a Fickean-type diffusion kinetics would be fulfilled, since the relaxation of the polymer chains is not the limiting step for swelling. Consequently, the experimental data had to show a linear dependence between the swelling and $t^{1/2}$. However, this is not the case either.

All of this analysis shows that along with the diffusion, another process besides swelling is taking place. In this sense, the Eyring equation [35,36] can provide information about the diffusion mechanism that takes place and sheds light on the causes of the observed negative values for the activation energies of the global diffusion process:

$$k = \frac{k_B T}{h} exp\left(-\frac{\Delta G^\ddagger}{RT}\right) \tag{4}$$

here k_B, h, and R are the Boltzmann, Planck, and the gas constants, respectively. The activation Gibbs free energy, $\Delta G^\ddagger$, is related to the activation enthalpy and entropy ($\Delta H^\ddagger$, $\Delta S^\ddagger$), according to the following expression:

$$\Delta G^\ddagger = \Delta H^\ddagger - T\Delta S^\ddagger \tag{5}$$

Then, substituting (5) in (4):

$$k = \frac{k_B T}{h} \, exp\left(\frac{\Delta S^{\ddagger}}{R}\right) exp\left(-\frac{\Delta H^{\ddagger}}{RT}\right) \tag{6}$$

which can be linearized as follows:

$$ln\frac{k}{T} = ln\frac{k_B}{h} + \frac{\Delta S^{\ddagger}}{R} - \frac{\Delta H^{\ddagger}}{R} \cdot \frac{1}{T} \tag{7}$$

This kinetic treatment describes the dependence of the rate of a chemical reaction with temperature when the concepts of statistical mechanics are applied. Even though this analysis is based on the theory of absolute reaction rates developed to treat ordinary chemical reactions, it was demonstrated that this model could be successfully used to describe the kinetic treatment of viscosity and diffusion [37,38].

In order to elucidate the mechanism that takes place during the diffusion of water through these aerogels using the statistical approach of Eyring, it is necessary to estimate the rate constants of the swelling process. The experimental data showed an excellent fit to the following Equation proposed by Schott [39]:

$$\frac{t}{W} = A + Bt \tag{8}$$

which describes a second-order kinetics with respect to the unrealized swelling:

$$\frac{dW}{dt} = k(W_{\infty} - W)^2 \tag{9}$$

and the kinetic constant becomes equal to:

$$k = \frac{1}{AW_{\infty}^2} \tag{10}$$

The calculated values of the second-order rate constant, k, are included in Table 3, and were used to perform a thermo-kinetic analysis according to the Eyring Equation (7), as shown in Figure 8. The excellent adjustment that is obtained is evident. In Table 4, the values of $\Delta H^{\ddagger}$, $\Delta S^{\ddagger}$, and $\Delta G^{\ddagger}$ are summarized.
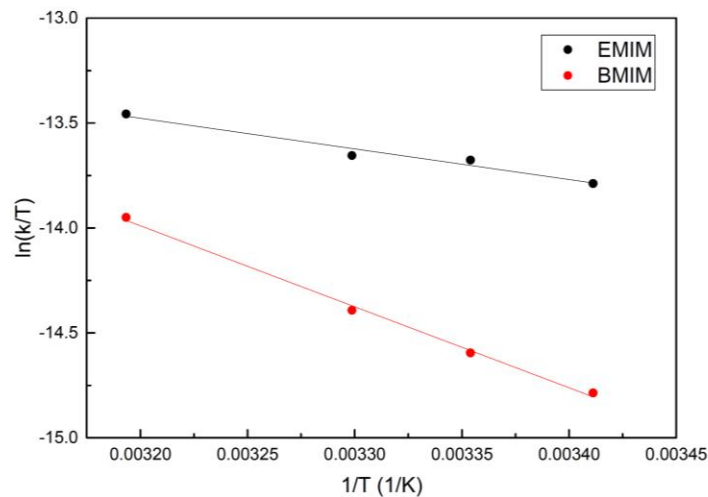
Figure 8. Plots of $\ln(k/T)$ versus $1/T$ using the second-order rate constants obtained from Equation (10) for the two aerogels.

Table 4. Activation energies calculated from D by the Arrhenius Equation (3). Thermo-kinetic parameters: $\Delta H^{\ddagger}$ and $\Delta S^{\ddagger}$ estimated from the Eyring Equation (7) and $\Delta G^{\ddagger}$ calculated at 298.15 K using the Equation (5).

Aerogel	Ea (kJ/mol)	$\Delta H^{\ddagger}$ (kJ/mol)	$\Delta S^{\ddagger}$ (J/mol·K)	$-T\Delta S^{\ddagger\,a}$ (kJ/mol)	$\Delta G^{\ddagger\,a}$ (kJ/mol)
CsE	−17.5	12.1	−271	80.7	92.9
CsB	−9.2	32.1	−211	63.0	95.1

[a] Evaluated at $T = 298.15$ K.

When analyzing the thermo-kinetic parameters, it is observed that the activation enthalpies are positive due to the endothermic change from starting intermediates to the transition state during the overall diffusion process. According to these activation parameters, at 298.15 K, the change of the activation Gibbs free energy is largely controlled by the activation entropy term (e.g., $-T\Delta S^{\ddagger}$ = 81 kJ/mol for the CsE aerogel), while the contribution of the activation enthalpy to the transition state is not so significant ($\Delta H^{\ddagger}$ = 12 kJ/mol). In this sense, it is important to note that these data indicate a significant increase in the order of the atoms that are involved during the pass to the transition state, with a small absorption of heat.

The values of these activation parameters are very similar to those that are observed during the formation of hydrogen bonds [40–42]. Their magnitudes coincide with the chemical nature of hydrogen bonding. Their formation involves relatively low energy and implicates the rearrangement of water molecules around the polymer, creating a hydration shell that is spatially oriented towards the hydroxyl and amino groups of chitosan.

At this point, it is important to remember that during the dissolution of chitosan in ionic liquids, the intra- and intermolecular hydrogen bonds of chitosan chains are broken. Although at the moment of forming the physical cross-linking the formation of some amount of hydrogen bonds is propitiated, these are relatively few in comparison with the large number of groups that are able to form hydrogen bonds in the polymer. In this way, during the swelling of the aerogels in water, along with the diffusion process, the generation of a huge amount of hydrogen bonds takes place with the consequent formation of a hydration shell. This analysis unambiguously supports the observed complex nature of the swelling processes of these aerogels, whose hydrated structure is apparently organized through hydrogen bonds. For this reason, a large contribution of $\Delta S^{\ddagger}$ to the transition state is appreciated, when compared to that of $\Delta H^{\ddagger}$.

4. Conclusions

Physical ionogels were obtained from chitosan solutions in EMIMAc and BMIMAc by non-solvent agent vapor diffusion (ethanol or water). The gels that were formed with ethanol treatment were rigid and brittle. Conversely, water vapor treatment only produce gels from the EMIMAc solution, these gels were too soft and brittle to be processed. Aerogels were produced by supercritical CO_2 drying using ionogels that were produced by ethanol treatment. Such aerogels were low density mesoporous materials with surface area between 350 and 480 m^2/g. There is neither spectroscopic evidence of changes in the chemical identity of the chitosan after aerogels production nor evidence of residual IL in the obtained materials. The internal structures of both types of aerogels were similar, appearing as mesoporous materials that are formed by agglomerated clumps.

The swelling of these aerogels followed a second-order kinetics. The application of the Eyring equation to the dependence of the rate constants on temperature allowed for clarifying the characteristics of the diffusion of water. The change of the activation Gibbs energy is mainly controlled by the activation entropy, rather than by the activation enthalpy at the tested temperatures. The kinetics of swelling seems to be controlled by the formation of hydrogen bonding, instead of the diffusion of water itself.

Aerogels with such characteristics have the potential for applications in the pharmaceutical industry as materials for the encapsulation, retention, and transport of model molecules that have affinities for chitosan. In the environmental field, these aerogels can be used as materials for the removal of pollutants from the effluents of industries in an extractive process by picking up minerals or compounds that are considered to be contaminants with affinity for chitosan. Another potential use is in the food industry or biotechnology, where components such as enzymes, proteins, or compounds that are part of a process could be immobilized inside the aerogels.

Author Contributions: Jaime Lizardi-Mendoza and Waldo Argüelles-Monal conceived and designed the experiments; Gonzalo Santos-López performed the experiments; Gonzalo Santos-López, Waldo Argüelles-Monal and Jaime Lizardi-Mendoza analyzed the data; Maricarmen T. Recillas-Mota, Yolanda L. López-Franco and Elizabeth Carvajal-Millan contributed with reagents, materials and analytical advice; Gonzalo Santos-López, Waldo Argüelles-Monal and Jaime Lizardi-Mendoza wrote the paper and all the authors contributed to discuss and review the paper.

Conflicts of Interest: The authors declare no conflict of interest. The founding sponsors had no role in the design of the study; in the collection, analyses, or interpretation of data; in the writing of the manuscript, and in the decision to publish the results.

References

1. Valentin, R.; Bonelli, B.; Garrone, E.; Di Renzo, F.; Quignard, F. Accessibility of the Functional Groups of Chitosan Aerogel Probed by FT-IR-Monitored Deuteration. *Biomacromolecules* **2007**, *8*, 3646–3650. [CrossRef] [PubMed]

2. Pohako-Esko, K.; Bahlmann, M.; Schulz, P.S.; Wasserscheid, P. Chitosan Containing Supported Ionic Liquid Phase Materials for CO_2 Absorption. *Ind. Eng. Chem. Res.* **2016**, *55*, 7052–7059. [CrossRef]

3. Guyomard-Lack, A.; Buchtová, N.; Humbert, B.; Bideau, J.L. Ion segregation in an ionic liquid confined within chitosan based chemical ionogels. *Phys. Chem. Chem. Phys.* **2015**, *17*, 23947–23951. [CrossRef] [PubMed]

4. Trivedi, T.J.; Rao, K.S.; Kumar, A. Facile preparation of agarose-chitosan hybrid materials and nanocomposite ionogels using an ionic liquid via dissolution, regeneration and sol-gel transition. *Green Chem.* **2014**, *16*, 320–330. [CrossRef]

5. Ma, B.; Li, X.; Qin, A.; He, C. A comparative study on the chitosan membranes prepared from glycine hydrochloride and acetic acid. *Carbohydr. Polym.* **2013**, *91*, 477–482. [CrossRef] [PubMed]

6. Kuzmina, O.; Heinze, T.; Wawro, D. Blending of Cellulose and Chitosan in Alkyl Imidazolium Ionic Liquids. *ISRN Polym. Sci.* **2012**, *2012*, 251950. [CrossRef]

7. Xiong, Y.; Wang, H.; Wu, C.; Wang, R. Preparation and characterization of conductive chitosan–ionic liquid composite membranes. *Polym. Adv. Technol.* **2012**, *23*, 1429–1434. [CrossRef]

8. Silva, S.S.; Santos, T.C.; Cerqueira, M.T.; Marques, A.P.; Reys, L.L.; Silva, T.H.; Caridade, S.G.; Mano, J.F.; Reis, R.L. The use of ionic liquids in the processing of chitosan/silk hydrogels for biomedical applications. *Green Chem.* **2012**, *14*, 1463–1470. [CrossRef]

9. Liu, Z.; Wang, H.; Liu, C.; Jiang, Y.; Yu, G.; Mu, X.; Wang, X. Magnetic cellulose–chitosan hydrogels prepared from ionic liquids as reusable adsorbent for removal of heavy metal ions. *Chem. Commun.* **2012**, *48*, 7350–7352. [CrossRef] [PubMed]

10. Naseeruteen, F.; Hamid, N.S.A.; Suah, F.B.M.; Ngah, W.S.W.; Mehamod, F.S. Adsorption of malachite green from aqueous solution by using novel chitosan ionic liquid beads. *Int. J. Biol. Macromol.* **2017**. [CrossRef] [PubMed]

11. Muzzarelli, R.A.A. Biomedical Exploitation of Chitin and Chitosan via Mechano-Chemical Disassembly, Electrospinning, Dissolution in Imidazolium Ionic Liquids, and Supercritical Drying. *Mar. Drugs* **2011**, *9*, 1510–1533. [CrossRef] [PubMed]

12. Silva, S.S.; Mano, J.F.; Reis, R.L. Ionic liquids in the processing and chemical modification of chitin and chitosan for biomedical applications. *Green Chem.* **2017**, *19*, 1208–1220. [CrossRef]

13. Silva, S.S.; Duarte, A.R.C.; Carvalho, A.P.; Mano, J.F.; Reis, R.L. Green processing of porous chitin structures for biomedical applications combining ionic liquids and supercritical fluid technology. *Acta Biomater.* **2011**, *7*, 1166–1172. [CrossRef] [PubMed]

14. Kasaai, M.R. Various Methods for Determination of the Degree of N-Acetylation of Chitin and Chitosan: A Review. *J. Agric. Food Chem.* **2009**, *57*, 1667–1676. [CrossRef] [PubMed]

15. Ottøy, M.H.; Vårum, K.M.; Smidsrød, O. Compositional heterogeneity of heterogeneously deacetylated chitosans. *Carbohydr. Polym.* **1996**, *29*, 17–24. [CrossRef]

16. Scherließ, R.; Buske, S.; Young, K.; Weber, B.; Rades, T.; Hook, S. In vivo evaluation of chitosan as an adjuvant in subcutaneous vaccine formulations. *Vaccine* **2013**, *31*, 4812–4819. [CrossRef] [PubMed]

17. Rinaudo, M.; Pavlov, G.; Desbrières, J. Solubilization of Chitosan in Strong Acid Medium. *Int. J. Polym. Anal. Charact.* **1999**, *5*, 267–276. [CrossRef]

18. Montembault, A.; Viton, C.; Domard, A. Rheometric study of the gelation of chitosan in aqueous solution without cross-linking agent. *Biomacromolecules* **2005**, *6*, 653–662. [CrossRef] [PubMed]

19. Le Bideau, J.; Viau, L.; Vioux, A. Ionogels, ionic liquid based hybrid materials. *Chem. Soc. Rev.* **2011**, *40*, 907–925. [CrossRef] [PubMed]

20. Cárdenas, A.; Argüelles-Monal, W.; Goycoolea, F.M.; Higuera-Ciapara, I.; Peniche, C. Diffusion through Membranes of the Polyelectrolyte Complex of Chitosan and Alginate. *Macromol. Biosci.* **2003**, *3*, 535–539. [CrossRef]

21. Seddon, K.R. Ionic Liquids for Clean Technology. *J. Chem. Technol. Biotechnol.* **1997**, *68*, 351–356. [CrossRef]

22. Chen, Y.; Sun, X.; Yan, C.; Cao, Y.; Mu, T. The Dynamic Process of Atmospheric Water Sorption in [EMIM][Ac] and Mixtures of [EMIM][Ac] with Biopolymers and CO_2 Capture in These Systems. *J. Phys. Chem. B* **2014**, *118*, 11523–11536. [CrossRef] [PubMed]

23. Vachoud, L.; Domard, A. Physicochemical properties of physical chitin hydrogels: Modeling and relation with the mechanical properties. *Biomacromolecules* **2001**, *2*, 1294–1300. [CrossRef] [PubMed]

24. Quignard, F.; Valentin, R.; Renzo, F.D. Aerogel materials from marine polysaccharides. *New J. Chem.* **2008**, *32*, 1300–1310. [CrossRef]

25. Subrahmanyam, R.; Gurikov, P.; Dieringer, P.; Sun, M.; Smirnova, I. On the Road to Biopolymer Aerogels—Dealing with the Solvent. *Gels* **2015**, *1*, 291–313. [CrossRef]

26. Brugnerotto, J.; Lizardi, J.; Goycoolea, F.M.; Argüelles-Monal, W.; Desbrieres, J.; Rinaudo, M. An infrared investigation in relation with chitin and chitosan characterization. *Polymer* **2001**, *42*, 3569–3580. [CrossRef]

27. Socrates, G. *Infrared and Raman Characteristic Group Frequencies: Tables and Charts*; John Wiley & Sons: Chichester, NY, USA, 2004; ISBN 978-0-470-09307-8.

28. Sing, K.S.W.; Everett, D.H.; Haul, R.A.W.; Moscou, L.; Pierotti, R.A.; Rouquerol, J.; Siemieniewska, T. Reporting Physisorption Data for Gas/Solid Systems. In *Handbook of Heterogeneous Catalysis*; Wiley-VCH Verlag GmbH & Co. KGaA: Weinheim, German, 2008; ISBN 978-3-527-61004-4.

29. Chang, X.; Chen, D.; Jiao, X. Chitosan-Based Aerogels with High Adsorption Performance. *J. Phys. Chem. B* **2008**, *112*, 7721–7725. [CrossRef] [PubMed]

30. Tsioptsias, C.; Stefopoulos, A.; Kokkinomalis, I.; Papadopoulou, L.; Panayiotou, C. Development of micro- and nano-porous composite materials by processing cellulose with ionic liquids and supercritical CO_2. *Green Chem.* **2008**, *10*, 965–971. [CrossRef]

31. Goycoolea, F.M.; Fernández-Valle, M.E.; Aranaz, I.; Heras, Á. pH- and Temperature-Sensitive Chitosan Hydrogels: Swelling and MRI Studies. *Macromol. Chem. Phys.* **2011**, *212*, 887–895. [CrossRef]

32. Crank, J. *The Mathematics of Diffusion*, 2nd ed.; Clarendon Press: Oxford, UK, 1979; ISBN 0-19-853411-6.

33. Vázquez, B.; San Roman, J.; Peniche, C.; Cohen, M.E. Polymeric Hydrophilic Hydrogels with Flexible Hydrophobic Chains. Control of the Hydration and Interactions with Water Molecules. *Macromolecules* **1997**, *30*, 8440–8446. [CrossRef]

34. Ritger, P.L.; Peppas, N.A. A simple equation for description of solute release I. Fickian and non-fickian release from non-swellable devices in the form of slabs, spheres, cylinders or discs. *J. Control. Release* **1987**, *5*, 23–36. [CrossRef]

35. Eyring, H. The Activated Complex in Chemical Reactions. *J. Chem. Phys.* **1935**, *3*, 107–115. [CrossRef]

36. Wynne-Jones, W.F.K.; Eyring, H. The Absolute Rate of Reactions in Condensed Phases. *J. Chem. Phys.* **1935**, *3*, 492–502. [CrossRef]

5. CONCLUSIONES Y RECOMENDACIONES

Se planteó una investigación enfocada en obtener aerogeles a partir de soluciones de quitosano en líquidos iónicos. Además de la generación de materiales novedosos a partir de las soluciones de quitosano en líquidos iónicos, se aporta conocimiento sobre la interacción del quitosano con los líquidos iónicos basados en imidazolio. Esto se llevó a cabo de tal forma que permitiera estudiar a fondo la disolución del quitosano en líquidos iónicos, con la finalidad de conocer y correlacionar los factores principales que influyen en el ordenamiento de las cadenas en la gelificación y que se reflejan en la estructura porosa de los aerogeles. Se empleó resonancia magnética nuclear de dominio de tiempo para analizar la dinámica molecular en las soluciones por medio de los parámetros de relajación de protones. Este análisis permitió reconocer la presencia de, al menos, dos poblaciones de protones que se comportan de manera distinta. De acuerdo con esto, una población estaría relacionada con especies de baja movilidad molecular –como el polímero– y componentes del solvente asociados a éstas, mientras que la otra población estaría relacionada con especies de bajo peso molecular, que no se ven afectadas por la presencia del quitosano. Este reporte es un aporte original para determinar la dinámica molecular y mecanismos de solvatación del quitosano disuelto en líquidos iónicos. Las soluciones de quitosano también fueron analizadas utilizando reología de baja deformación para determinar los parámetros de flujo y la viscosidad intrínseca del quitosano en líquidos iónicos. A partir de las curvas de flujo se observó que el quitosano se comporta como un fluido newtoniano a bajas concentraciones, pero al aumentar la concentración la viscosidad varía con la tasa de corte comportándose como fluido no newtoniano. Similares resultados han sido reportados para celulosa utilizando los mismos líquidos iónicos, lo que indicaría mecanismos de solvatación semejantes del quitosano en líquidos iónicos. El análisis de las curvas de flujo permitió reportar por primera vez, el valor de la viscosidad intrínseca del quitosano en líquidos, la cual es proporcional al volumen hidrodinámico. Los valores obtenidos indican que la molécula de quitosano adopta una conformación más compacta y flexible en líquidos iónicos que los reportados para solventes ácidos acuosos. Este trabajo de tesis es un aporte original

para el conocimiento del quitosano en este tipo de soluciones. La segunda parte del trabajo se enfocó en obtener y caracterizar los materiales porosos nanoestructurados. Se diseñó la forma de producir geles físicos de quitosano en líquidos iónicos mediante la difusión de vapor de agentes no solventes como alcohol y agua, sin emplear agentes entrecruzantes añadidos. Los ionogeles obtenidos resultaron firmes y traslucidos. A partir de estos ionogeles se ideó la forma de producir aerogeles, los cuales resultaron tener alta área superficial específica y mesoporosidad. El proceso de formación de los ionogeles y aerogeles no modificó la composición química del quitosano. La estructura interna de los aerogeles se observó en forma de agregados compactos, los cuales pueden diferenciarse de los aerogeles de quitosano obtenidos a partir de soluciones ácidas acuosas. Dicha diferencia indica que las variaciones en la estructura interna de los aerogeles están relacionadas con las interacciones de las moléculas de quitosano con el solvente en el proceso de gelificación. Este es el primer reporte de aerogeles de quitosano obtenidos a partir de soluciones con líquidos iónicos lo cual ubica está investigación en la frontera de conocimiento en el tema. Las características observadas en los aerogeles los posicionan como materiales con un gran potencial de aplicación en áreas como la biotecnología, medicina, agricultura, ambiental y alimentos, entre otras. Este potencial se podrá detallar o determinar con la investigación de la funcionalidad de dichos materiales. Existe la posibilidad de generar tanto geles como aerogeles con diferente morfología, tales como microesferas de tamaño micro o nanométrico, además de fibras, películas, membranas y andamiajes a partir de soluciones con líquido iónico, ampliando el espectro de aplicación y generación de nuevos materiales.

6. REFERENCIAS BIBLIOGRÁFICAS

Agnihotri, S. A., Mallikarjuna, N. N. and Aminabhavi, T. M. 2004. Recent advances on chitosan-based micro- and nanoparticles in drug delivery. Journal of Controlled Release 100(1): 5-28.

Aranaz, I., Mengibar, M., Harris, R., Panos, I., Miralles, B., Acosta, N., Galed, G. and Heras, A. Functional Characterization of Chitin and Chitosan. Current Chemical Biology 3(2): 203-230.

Argüelles-Monal, W., Goycoolea, F. M., Peniche, C. and Higuera-Ciapara, I. 1998. Rheological study of the chitosan/glutaraldehyde chemical gel system. Polymer Gels and Networks 6(6): 429-440.

Argüelles-Monal, W., Heras, C. A., Acosta, N., Galed, G., Gallardo, A., Miralles, B., Peniche, C. and San Roman, J. 2004. Caracterización de quitina y quitosano. En: de Abram, A. P. (ed.). Quitina y Quitosano: obtención, caracterización y aplicaciones. Fondo Editorial de la Pontifícia Universidad Católica del Peru Lima, Peru: 157-206.

Beaney, P., Lizardi-Mendoza, J. and Healy, M. 2005. Comparison of chitins produced by chemical and bioprocessing methods. Journal of Chemical Technology & Biotechnology 80(2): 145-150.

Benedetto, A. and Ballone, P. 2016. Room Temperature Ionic Liquids Meet Biomolecules: A Microscopic View of Structure and Dynamics. ACS Sustainable Chemistry & Engineering 4(2): 392-412.

Berger, J., Reist, M., Mayer, J. M., Felt, O., Peppas, N. A. and Gurny, R. 2004. Structure and interactions in covalently and ionically crosslinked chitosan hydrogels for biomedical applications. Eur J Pharm Biopharm 57(1): 19-34.

Bogolitsyn, K. G., Skrebets, T. E. and Makhova, T. A. 2009. Physicochemical properties of 1-butyl-3-methylimidazolium acetate. Russian Journal of General Chemistry 79(1): 125-128.

Brugnerotto, J., Lizardi, J., Goycoolea, F. M., Argüelles-Monal, W., Desbrières, J. and Rinaudo, M. 2001. An infrared investigation in relation with chitin and chitosan characterization. Polymer 42(8): 3569-3580.

Cárdenas, A., Argüelles-Monal, W., Goycoolea, F. M., Higuera-Ciapara, I. and Peniche, C. 2003. Diffusion Through Membranes of the Polyelectrolyte Complex of Chitosan and Alginate. Macromolecular Bioscience 3(10): 535-539.

Crank, J. 1978. The Mathematics of Diffusion.

Chang, X., Chen, D. and Jiao, X. 2008. Chitosan-based aerogels with high adsorption performance. J Phys Chem B 112(26): 7721-7725.

Chen, Q., Xu, A., Li, Z., Wang, J. and Zhang, S. 2011. Influence of anionic structure on the dissolution of chitosan in 1-butyl-3-methylimidazolium-based ionic liquids. Green Chemistry 13(12): 3446-3452.

Chen, Y., Sun, X., Yan, C., Cao, Y. and Mu, T. 2014. The Dynamic Process of Atmospheric Water Sorption in [EMIM][Ac] and Mixtures of [EMIM][Ac] with Biopolymers and CO2 Capture in These Systems. The Journal of Physical Chemistry B.

Dash, M., Chiellini, F., Ottenbrite, R. M. and Chiellini, E. 2011. Chitosan--A versatile semi-synthetic polymer in biomedical applications. Progress in Polymer Science 36(8): 981-1014.

El Seoud, O. A., Koschella, A., Fidale, L. C., Dorn, S. and Heinze, T. 2007. Applications of Ionic Liquids in Carbohydrate Chemistry: A Window of Opportunities. Biomacromolecules 8(9): 2629-2647.

Eyring, H. 1935. The Activated Complex in Chemical Reactions. The Journal of Chemical Physics 3(2): 107-115.

Eyring, H. 1936. Viscosity, Plasticity, and Diffusion as Examples of Absolute Reaction Rates. The Journal of Chemical Physics 4(4): 283-291.

Ferry, J. D. 1961. Viscoelastic properties of polymers, Wiley.

Geng, X., Kwon, O.-H. and Jang, J. 2005. Electrospinning of chitosan dissolved in concentrated acetic acid solution. Biomaterials 26(27): 5427-5432.

Gericke, M., Schlufter, K., Liebert, T., Heinze, T. and Budtova, T. 2009. Rheological Properties of Cellulose/Ionic Liquid Solutions: From Dilute to Concentrated States. Biomacromolecules 10(5): 1188-1194.

Gooday, G. W. 1990. The Ecology of Chitin DegradationEn: Marshall, K. C. (ed.). Advances in Microbial Ecology. Springer US Boston, MA**:** 387-430

Goycoolea F., A. E., Mato R., Ed. (2004). Caracterización de quitina y quitosano. Capítulo 3, *Fuentes y procesos de obtención*. Lima, Peru, Fondo Editorial de la Pontifícia Universidad Católica del Peru.

Goycoolea, F. M., Fernández-Valle, M. E., Aranaz, I. and Heras, Á. 2011. pH- and Temperature-Sensitive Chitosan Hydrogels: Swelling and MRI Studies. Macromolecular Chemistry and Physics: n/a-n/a.

Graessley, W. 1974. The entanglement concept in polymer rheology(ed.). The Entanglement Concept in Polymer Rheology. Springer Berlin Heidelberg, 16**:** 1-179.

Guyomard-Lack, A., Buchtova, N., Humbert, B. and Le Bideau, J. 2015. Ion segregation in an ionic liquid confined within chitosan based chemical ionogels. Physical Chemistry Chemical Physics.

Hallett, J. P. and Welton, T. 2011. Room-Temperature Ionic Liquids: Solvents for Synthesis and Catalysis. 2. Chemical Reviews 111(5): 3508-3576.

Heatley, F. 1979. Nuclear magnetic relaxation of synthetic polymers in dilute solution. Progress in Nuclear Magnetic Resonance Spectroscopy 13(1): 47-85.

Ishizuka, T., Ohzu, S., Kotani, H., Shiota, Y., Yoshizawa, K. and Kojima, T. 2014. Hydrogen atom abstraction reactions independent of C-H bond dissociation energies of organic substrates in water: significance of oxidant-substrate adduct formation. Chemical Science 5(4): 1429-1436.

Kasaai, M. R. 2009. Various Methods for Determination of the Degree of N-Acetylation of Chitin and Chitosan: A Review. Journal of Agricultural and Food Chemistry 57(5): 1667-1676.

Keskin, S., Kayrak-Talay, D., Akman, U. and Hortaçsu, Ö. 2007. A review of ionic liquids towards supercritical fluid applications. The Journal of Supercritical Fluids 43(1): 150-180.

Kincaid, J. F., Eyring, H. and Stearn, A. E. 1941. The Theory of Absolute Reaction Rates and its Application to Viscosity and Diffusion in the Liquid State. Chemical Reviews 28(2): 301-365.

Kuzmina, O., Heinze, T. and Wawro, D. 2012. Blending of Cellulose and Chitosan in Alkyl Imidazolium Ionic Liquids. ISRN Polymer Science 2012: 9.

Lavertu, M., Xia, Z., Serreqi, A. N., Berrada, M., Rodrigues, A., Wang, D., Buschmann, M. D. and Gupta, A. 2003. A validated 1H NMR method for the determination of the degree of deacetylation of chitosan. Journal of Pharmaceutical and Biomedical Analysis 32(6): 1149-1158.

Le Bideau, J., Viau, L. and Vioux, A. 2011. Ionogels, ionic liquid based hybrid materials. Chemical Society Reviews 40(2): 907-925.

Liu, H., Sale, K. L., Holmes, B. M., Simmons, B. A. and Singh, S. 2010. Understanding the Interactions of Cellulose with Ionic Liquids: A Molecular Dynamics Study. The Journal of Physical Chemistry B 114(12): 4293-4301.

Liu, Z., Wang, H., Liu, C., Jiang, Y., Yu, G., Mu, X. and Wang, X. 2012. Magnetic cellulose-chitosan hydrogels prepared from ionic liquids as reusable adsorbent for removal of heavy metal ions. Chemical Communications 48(59): 7350-7352.

Lizardi-Mendoza, J. 2007. Structured Porous Materials of Chitin and Chitosan. Doctor of Philosophy, Queen's University Belfast.

Lizardi-Mendoza, J., Argüelles Monal, W. M. and Goycoolea Valencia, F. M. 2016. Chapter 1 - Chemical Characteristics and Functional Properties of Chitosan A2 - Bautista-Baños, SilviaEn: Romanazzi, G. and A. Jiménez-Aparicio (ed.). Chitosan in the Preservation of Agricultural Commodities. Academic Press San Diego**:** 3-31.

Long, D. A. 2004. Infrared and Raman characteristic group frequencies. Tables and charts George Socrates John Wiley and Sons, Ltd, Chichester, Third Edition, 2001. Price £135. Journal of Raman Spectroscopy 35(10): 905-905.

Ma, B., Li, X., Qin, A. and He, C. 2013. A comparative study on the chitosan membranes prepared from glycine hydrochloride and acetic acid. Carbohydrate Polymers 91(2): 477-482.

Matveev, V. V., Markelov, D. A., Brui, E. A., Chizhik, V. I., Ingman, P. and Lahderanta, E. 2014. 13C NMR relaxation and reorientation dynamics in imidazolium-based ionic liquids: revising interpretation. Physical Chemistry Chemical Physics 16(22): 10480-10484.

Montembault, A., Viton, C. and Domard, A. 2005. Rheometric Study of the Gelation of Chitosan in Aqueous Solution without Cross-Linking Agent. Biomacromolecules 6(2): 653-662.

Morris, E. R., Cutler, A. N., Ross-Murphy, S. B., Rees, D. A. and Price, J. 1981. Concentration and shear rate dependence of viscosity in random coil polysaccharide solutions. Carbohydrate Polymers 1(1): 5-21.

Murugesan, S. and Linhardt, R. J. 2005. Ionic Liquids in Carbohydrate Chemistry - Current Trends and Future Directions. Current Organic Synthesis 2(4): 437-451.

Muzzarelli, R. A. A. 1977. Chapter 1 - Enzymic synthesis of chitin and chitosan(ed.). Chitin. Pergamon**:** 5-44.

Naseeruteen, F., Hamid, N. S. A., Suah, F. B. M., Ngah, W. S. W. and Mehamod, F. S. 2018. Adsorption of malachite green from aqueous solution by using novel chitosan ionic liquid beads. International Journal of Biological Macromolecules 107: 1270-1277.

Nazet, A., Sokolov, S., Sonnleitner, T., Makino, T., Kanakubo, M. and Buchner, R. 2015. Densities, Viscosities, and Conductivities of the Imidazolium Ionic Liquids [Emim][Ac], [Emim][FAP], [Bmim][BETI], [Bmim][FSI], [Hmim][TFSI], and [Omim][TFSI]. Journal of Chemical & Engineering Data 60(8): 2400-2411.

Novoa-Carballal, R., Fernandez-Megia, E. and Riguera, R. 2010. Dynamics of Chitosan by 1H NMR Relaxation. Biomacromolecules 11(8): 2079-2086.

Ottey, M. H., Vårum, K. M. and Smidsrød, O. 1996. Compositional heterogeneity of heterogeneously deacetylated chitosans. Carbohydrate Polymers 29(1): 17-24.

Pauling, L. 1960. The Nature of the Chemical Bond and the Structure of Molecules and Crystals: An Introduction to Modern Structural Chemistry, Cornell University Press.

Peppas, N. A. 1987. Hydrogels in Medicine and Pharmacy: Properties and applications, CRC Press.

Pohako-Esko, K., Bahlmann, M., Schulz, P. S. and Wasserscheid, P. 2016. Chitosan Containing Supported Ionic Liquid Phase Materials for CO2 Absorption. Industrial & Engineering Chemistry Research 55(25): 7052-7059.

Prabhumirashi, L. S. and Jose, C. I. 1975. Infra-red studies and thermodynamics of hydrogen bonding in ethylene glycol monoalkyl ethers. Evidence for a ten membered ring dimer. Journal of the Chemical Society, Faraday Transactions 2: Molecular and Chemical Physics 71(0): 1545-1554.

Qin, Y., Lu, X., Sun, N. and Rogers, R. D. 2010. Dissolution or extraction of crustacean shells using ionic liquids to obtain high molecular weight purified chitin and direct production of chitin films and fibers. Green Chemistry 12(6): 968-971.

Quignard, F., Valentin, R. and Di Renzo, F. 2008. Aerogel materials from marine polysaccharides. New Journal of Chemistry 32(8): 1300.

Raymond, L., Morin, F. G. and Marchessault, R. H. 1993. Degree of deacetylation of chitosan using conductometric titration and solid-state NMR. Carbohydrate Research 246(1): 331-336.

Remsing, R. C., Hernandez, G., Swatloski, R. P., Massefski, W. W., Rogers, R. D. and Moyna, G. 2008. Solvation of Carbohydrates in N,N′-Dialkylimidazolium Ionic Liquids: A Multinuclear NMR Spectroscopy Study. The Journal of Physical Chemistry B 112(35): 11071-11078.

Rinaudo, M. 2006. Chitin and chitosan: Properties and applications. Progress in Polymer Science 31(7): 603-632.

Rinaudo, M., Milas, M. and Le Dung, P. 1993. Characterization of chitosan. Influence of ionic strength and degree of acetylation on chain expansion. Int J Biol Macromol 15(5): 281-285.

Rinaudo, M., Pavlov, G. and Desbrières, J. 1999. Influence of acetic acid concentration on the solubilization of chitosan. Polymer 40(25): 7029-7032.

Rinaudo, M., Pavlov, G. and Desbrières, J. 1999. Solubilization of Chitosan in Strong Acid Medium. International Journal of Polymer Analysis and Characterization 5(3): 267-276.

Ritger, P. L. and Peppas, N. A. 1987. A simple equation for description of solute release II. Fickian and anomalous release from swellable devices. Journal of Controlled Release 5(1): 37-42.

Roberts, G. A. F. 2005. A novel solvent system for chitosan, Advances in Chitin Science Vol. VIII. Poznan.

Rudaz, C. and Budtova, T. 2013. Rheological and hydrodynamic properties of cellulose acetate/ionic liquid solutions. Carbohydrate Polymers 92(2): 1966-1971.

Sahu, A., Goswami, P. and Bora, U. 2009. Microwave mediated rapid synthesis of chitosan. Journal of Materials Science: Materials in Medicine 20(1): 171-175.

Santos-López, G., Argüelles-Monal, W., Carvajal-Millan, E., López-Franco, Y. L., Recillas-Mota, M. T. and Lizardi-Mendoza, J. 2017. Aerogels from Chitosan Solutions in Ionic Liquids. Polymers 9: 722.

Scherließ, R., Buske, S., Young, K., Weber, B., Rades, T. and Hook, S. 2013. In vivo evaluation of chitosan as an adjuvant in subcutaneous vaccine formulations. Vaccine 31(42): 4812-4819.

Schott, H. 1992. Swelling kinetics of polymers. Journal of Macromolecular Science, Part B 31(1): 1-9.

Seddon, K. R. 1997. Ionic Liquids for Clean Technology. Journal of Chemical Technology & Biotechnology 68(4): 351-356.

Sescousse, R., Le, K. A., Ries, M. E. and Budtova, T. 2010. Viscosity of Cellulose−Imidazolium-Based Ionic Liquid Solutions. The Journal of Physical Chemistry B 114(21): 7222-7228.

Shen, X., Shamshina, J. L., Berton, P., Gurau, G. and Rogers, R. D. 2016. Hydrogels based on cellulose and chitin: fabrication, properties, and applications. Green Chemistry 18(1): 53-75.

Silva, S. S., Duarte, A. R. C., Carvalho, A. P., Mano, J. F. and Reis, R. L. 2011. Green processing of porous chitin structures for biomedical applications combining ionic liquids and supercritical fluid technology. Acta Biomaterialia 7: 1166-1172.

Silva, S. S., Mano, J. F. and Reis, R. L. 2017. Ionic liquids in the processing and chemical modification of chitin and chitosan for biomedical applications. Green Chemistry 19(5): 1208-1220.

Silva, S. S., Santos, T. C., Cerqueira, M. T., Marques, A. P., Reys, L. L., Silva, T. H., Caridade, S. G., Mano, J. F. and Reis, R. L. 2012. The use of ionic liquids in the processing of chitosan/silk hydrogels for biomedical applications. Green Chemistry 14(5): 1463-1470.

Sing, K. S. W., Everett, D. H., Haul, R. A. W., Moscou, L., Pierotti, R. A., Rouquerol, J. and Siemieniewska, T. 2008. Reporting Physisorption Data for Gas/Solid Systems(ed.). Handbook of Heterogeneous Catalysis. Wiley-VCH Verlag GmbH & Co. KGaA.

Socrates, G. 2001. Infrared and Raman Characteristic Group Frequencies: Tables and Charts, Wiley.

Sorlier, P., Denuzière, A., Viton, C. and Domard, A. 2001. Relation between the Degree of Acetylation and the Electrostatic Properties of Chitin and Chitosan. Biomacromolecules 2(3): 765-772.

Subrahmanyam, R., Gurikov, P., Dieringer, P., Sun, M. and Smirnova, I. 2015. On the Road to Biopolymer Aerogels—Dealing with the Solvent. Gels 1: 291-313.

Sun, X., Tian, Q., Xue, Z., Zhang, Y. and Mu, T. 2014. The dissolution behaviour of chitosan in acetate-based ionic liquids and their interactions: from experimental evidence to density functional theory analysis. RSC Advances 4(57): 30282-30291.

Swatloski, R. P., Spear, S. K., Holbrey, J. D. and Rogers, R. D. 2002. Dissolution of Cellose with Ionic Liquids. Journal of the American Chemical Society 124(18): 4974-4975.

Tariq, M., Forte, P. A. S., Gomes, M. F. C., Lopes, J. N. C. and Rebelo, L. P. N. 2009. Densities and refractive indices of imidazolium- and phosphonium-based ionic liquids: Effect of temperature, alkyl chain length, and anion. The Journal of Chemical Thermodynamics 41(6): 790-798.

Trivedi, T. J., Rao, K. S. and Kumar, A. 2014. Facile preparation of agarose-chitosan hybrid materials and nanocomposite ionogels using an ionic liquid via dissolution, regeneration and sol-gel transition. Green Chemistry 16(1): 320-330.

Tsioptsias, C., Stefopoulos, A., Kokkinomalis, I., Papadopoulou, L. and Panayiotou, C. 2008. Development of micro- and nano-porous composite materials by processing cellulose with ionic liquids and supercritical CO2. Green Chemistry 10: 965-971.

Vachoud, L. and Domard, A. 2001. Physicochemical Properties of Physical Chitin Hydrogels: Modeling and Relation with the Mechanical Properties. Biomacromolecules 2(4): 1294-1300.

Valentin, R., Bonelli, B., Garrone, E., Di Renzo, F. and Quignard, F. 2007. Accessibility of the functional groups of chitosan aerogel probed by FT-IR-monitored deuteration. Biomacromolecules 8(11): 3646-3650.

Vázquez, B., San Roman, J., Peniche, C. and Cohen, M. E. 1997. Polymeric Hydrophilic Hydrogels with Flexible Hydrophobic Chains. Control of the Hydration and Interactions with Water Molecules. Macromolecules 30(26): 8440-8446.

Wang, H., Gurau, G. and Rogers, R. D. 2012. Ionic liquid processing of cellulose. Chemical Society Reviews 41: 1519-1537.

Wang, W., Bo, S., Li, S. and Qin, W. 1991. Determination of the Mark-Houwink equation for chitosans with different degrees of deacetylation. International Journal of Biological Macromolecules 13(5): 281-285.

Wang, Z., Zheng, L., Li, C., Zhang, D., Xiao, Y., Guan, G. and Zhu, W. 2013. A novel and simple procedure to synthesize chitosan-graft-polycaprolactone in an ionic liquid. Carbohydrate Polymers 94(1): 505-510.

Wu, Y., Sasaki, T., Irie, S. and Sakurai, K. 2008. A novel biomass-ionic liquid platform for the utilization of native chitin. Polymer 49(9): 2321-2327.

Wynne-Jones, W. F. K. and Eyring, H. 1935. The Absolute Rate of Reactions in Condensed Phases. The Journal of Chemical Physics 3(8): 492-502.

Xie, H., Zhang, S. and Li, S. 2006. Chitin and chitosan dissolved in ionic liquids as reversible sorbents of CO2. Green Chemistry 8(7): 630-633.

Xiong, Y., Wang, H., Wu, C. and Wang, R. 2012. Preparation and characterization of conductive chitosan–ionic liquid composite membranes. Polymers for Advanced Technologies 23(11): 1429-1434.

Xu, B., Li, Q., Zhuang, L., Wang, Q., Li, C., Wang, G., Xie, F. and Halley, P. J. 2016. Dissolution and regeneration behavior of chitosan in 3-methyl-1-(ethylacetyl)imidazolium chloride. Fibers and Polymers 17(11): 1741-1748.